IMPROVED RESERVOIR CHARACTERIZATION AND SIMULATION OF A MATURE FIELD USING AN INTEGRATED APPROACH

By

WOAN JING TEH

Submitted to the graduate degree program in Chemical & Petroleum Engineering and the Graduate Faculty of the University of Kansas in partial fulfillment of the requirements for the degree of Master of Science.

_____

Chair of Committee: Dr. G Paul Willhite

_____

Dr. John H Doveton

_____

Dr. Shapour Vossoughi

Date Defended: June 1, 2012

The Thesis Committee for Woan Jing Teh
certifies that this is the approved version of the following thesis:

IMPROVED RESERVOIR CHARACTERIZATION AND SIMULATION
OF A MATURE FIELD USING AN INTEGRATED APPROACH

_____

Chair of Committee: Dr G. Paul Willhite

Date approved: June 1, 2012

ABSTRACT

Reservoir characterization involves various studies which comprises assimilation and interpretation of representative reservoir rock and fluid data for a simulation model under varying recovery mechanisms. The main challenge in reservoir simulation is the task of simplifying complex reservoir situations while ensuring a high level of data utilization to obtain a unique solution for history matching. Retaining geologic continuity in the simulation model is necessary to ensure the predictive capability of the reservoir model. In this study, the systematic assignment of reservoir properties with optimal utilization of very limited data has ensured that the fluid movement through the heterogeneous reservoir rock in a mature field is appropriately established. The key towards such a systematic assignment is classification of pore attributes. Pore attributes, which occur due to variations in depositional environments and diagenetic processes in a reservoir, have been identified through interpretation of the petrophysical data and the development of core- well log relationships in a consistent manner. Electrofacies along with petrophysical classification methods have been applied to quantify heterogeneity found in carbonate and sandstone reservoirs. It is observed that the electrofacies derived from well logs represent lithofacies found in the core measurements. The characterization approach has been shown to provide reliable accuracy of petrophysical property prediction when comparison was made with core measurements. These optimum correlation models were extended to uncored wells to describe the reservoir simulation model. A reservoir simulation model, built using this approach, provides a rapid means for history matching between the simulated results and the observed productions at the field while retaining the geological continuity. The integrated approach and structured methodology developed in this study resulted in a reservoir simulation model with adequate resolution of data that simulated the production history with sufficient realism, without necessity for alternations in petrophysical properties.

ACKNOWLEDGEMENTS

This study would not have been possible without the guidance and the help of many who have contributed and extended their valuable assistance. I would like to express my sincere thanks to them.

Dr. G. Paul Willhite, Ross H. Forney Distinguished Professor, Department of Chemical and Petroleum Engineering, for his patience, guidance and unfailing support as my advisor and mentor;

Dr. John H. Doveton, Senior Scientist at the Kansas Geological Survey, for his guidance and the insights he has shared;

Dr. Don W. Green, Deane E. Ackers Distinguished Professor, Department of Chemical and Petroleum Engineering, and Dr. Marylee Southard, for their concern and consideration to my academic needs;

Dr. Shapour Vossoughi, Dr. Jenn-Tai Liang, Dr. Jyun-Syung Tsau, Mark Ballard, staff at Tertiary Oil Recovery Project (TORP), staff at the Publications and Library Services of Kansas Geological Survey for rendering their help during the period of my study;

Dr. Christine Jensen Sundstrom, Director and Instructor of the Graduate Writing Program (GWP), for her encouragement to complete this study;

Dr. Glen A. Marotz, Associate Dean, Anna Paradis, Engineering Research and Graduate Programs, Carol Miner, for providing help regarding my academic requirement;

My colleagues, Ryan Berry and staff in the Chemical and Petroleum Engineering Department, for their assistance in the use of facilities;

Last but not the least, I wish to express my gratitude to my grandparents, parents, sisters and friends, for their love and support.

TABLE OF CONTENT

LIST OF FIGURES

LIST OF TABLES

CHAPTER 1

INTRODUCTION

1.1 Introduction

Reservoir description and characterization are important tools to provide a reliable reservoir model for flow simulation, assess the performance of a field, and eventually minimize cost and improve productivity of hydrocarbons. The reliability of the reservoir description depends upon the availability and uncertainty in data and also the procedures or guidelines used for collecting, interpreting and assigning reservoir description. The uncertainly in the reservoir model can be reduced when the reservoir description is improved with integration of various available data ranging from static data like geological information obtained from laboratory analyses as well as geologic studies to dynamic fluid flow data like field production. For reservoir simulation, especially for enhanced oil recovery, it is necessary that the heterogeneity in the petrophysical properties should honor field data for accurate flow simulation. In recent times, a number of data correlation and integration techniques (Yang, 1997;Vasco et al., 1999;Guerreiro et al., 2000;Hoffman and Kovscek, 2003;Subbey et al., 2004;Todd Hoffman and Caers, 2005;Caers et al., 2006;Huang et al., 2011) with some assessment of uncertainty have been proposed to improve the estimation of the reservoir properties, such as porosity, permeability, saturation etc. Integrated data models maintain geologic continuity, which gives them high predictive power in history matching as compared to traditional approaches. This thesis presents a methodology for characterization and simulation of large heterogeneous reservoirs with limited data. The objectives of this thesis are as follows: a) Understand and quantify the heterogeneity and distribution of petrophysical properties that represent the character of the reservoir b) Develop methods to obtain the aforementioned properties for constructing the reservoir and c) Demonstrate that the proposed method has obvious practical advantages in history-matching. This chapter provides an overview of the approach used in this thesis for building the reservoir model and simulating the production history.

The reservoir characterization begins with estimating the petrophysical properties for core and well log measurements. Porosity is calculated from resistivity logs using cementation exponents and permeability is calculated from porosity using petrophysical classifiers. We first introduce the theory that relates the cementation factor and petrophysical classifiers with the variation of pore structures observed from the core data. We then classify the well logs into electrofacies, to group similar lithofacies together. Subsequent well-log-core relationships of porosity and permeability are developed separately within each electrofacies and used to estimate petrophysical properties from well logs in uncored wells. A hybrid

approach is used for the spatial modeling of petrophysical property population. First, the dominant lithofacies and petrophysical property correlations are identified in their depositional environment and then the geostatistical procedure is applied separately for each lithofacies to maintain the lateral and vertical continuity in the geologic environment. The petrophysical propreties estimated along from well-logs are populated across the field using variograms followed by Sequential Gaussian Simulation. An attempt has been made to best integrate the information from geophysics, log-analysis, geology and engineering data.

Integrating the reservoir information into a reservoir model is a nontrivial process because reconciliation of different sources of information involves different scale of heterogeneities and degree of precision in spatial modeling. The history matching process of the production data gives an estimate of the large-scale distribution and continuity of petrophysical properties in the reservoir. However, the model architecture obtained from history matching will be predictive only if it can be obtained by upscaling the small-scale measurements from well logs. Sensitivity studies are carried out to determine the reservoir parameters, which have the greatest impact towards the simulation results. The sensitivity studies are followed by parameter adjustments in the reservoir model made according to the constraints dictated by the operating conditions. Two example applications described below illustrate the used of simplified architecture of the reservoir for history matching. We applied conventional reservoir modeling technique to the Ogallah field in Kansas, which presented a difficult problem to perform the production history matching. The example helps to identify data problems, which are most crucial to address before proceeding with more detailed analysis.

1.2 Preliminary Study

Simple reservoir models are necessary to generate a quick understanding to guide exploration and production operation. A simple model with large uncertainty in reservoir properties may be used for a first study of the reservoir performance. Typically, such a model can give a gross understanding of the reservoir drive mechanisms, but may necessitate unrealistic alterations of petrophysical properties in order to achieve a closer history match, especially at a more local scale. The preliminary simulation for a gross history match is performed using a rough estimate of permeability and large adjustments, if necessary. At this stage, it is attempted to bring all the history-matching dependent variables, such as pressure, water arrival time, to within tight tolerances. Two example applications described below will

illustrate the use of simplified reservoir models of the Ogallah field, which presented difficulty in history matching due to the critical heterogeneity of the reservoir being averaged out.

These examples involve the use of 3D models to simulate production from 2 overlaying carbonate-sandstone reservoirs called Arbuckle group as reported by Franseen (2004). The structure is almost an elliptical anticline trending northwest to southeast. The reservoirs communicate vertically and are supported by an underlying aquifer. Vugs and impermeable shale barrier are reported in the vicinity of the structure crest. The permeability and porosity relationship of the principal rock type is taken from the study of Byrnes et al. (1999) as seen in Fig. 1.1. To represent the field producing mechanism of bottom water drive, an aquifer is modeled using Carter-Tracey method at the bottom of the reservoir. Table 1.1 provides the data to describe the initial condition of the simulation model. Relative permeability curves of the field were approximated using Corey correlation. Fig. 1.1 shows the oil-water relative permeability curves being used which is the power law of the water saturation.

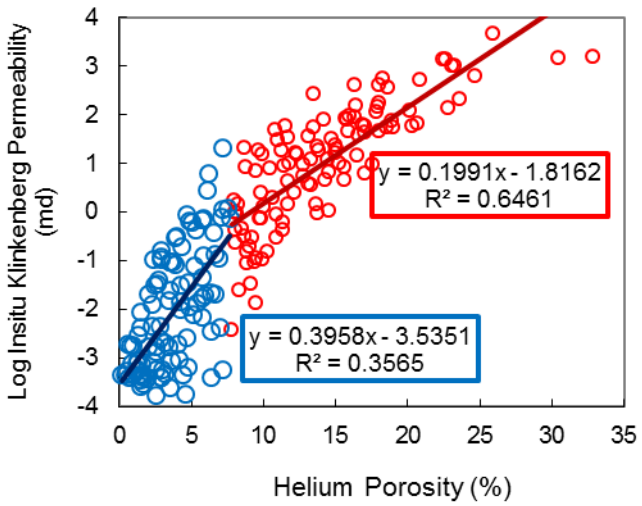

Fig. 1.1 - Arbuckle permeability-porosity relationship (Byrnes et al., 1999)

Table 1.1 - Formation Properties	
Original pressure, psia	1200
Temperature, ^{0}F	110
Oil gravity, API	36
Porosity, %	16 - 19
Permeability, md	50 - 260
Oil Water contact, ft	1715

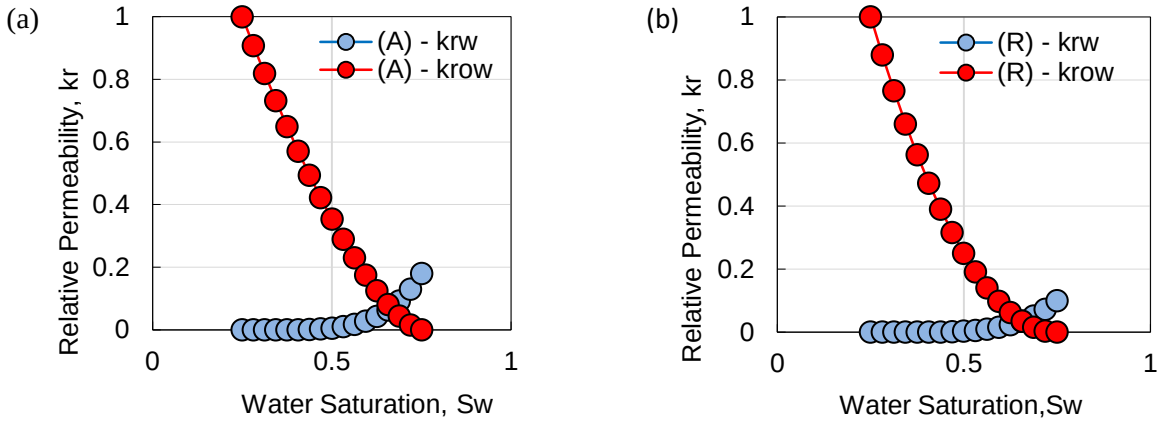

Fig. 1.2 - Oil-water relative permeability curves: (a) Arbuckle dolomite. (b) Reagan sandstone.

1.2.1 First Regression Trial

An 8 layer model of 118 x 125 x 6 blocks (42939 gridblocks) as shown in Fig. 1.3 was developed. The areal grid contains 103 wells. The simulated production period is continued from 1951 to 2009. We considered an infilled well (well 4-16) drilled in 1990 as the reference well that can provide reliable petrophysical properties for the reservoir model. The infill well was logged with modern-logs and the neutron and density logs obtained from the well were used to calibrate the porosity derived from the microlog. The neutron density porosity was cross-plotted with the microlog porosity to establish a correlation between them.

The porosity profiles of the wells were estimated using the transform porosity reported from microlog porosity as shown in Fig. 1.4. These porosity profiles are used in Archie equation to calculate the water saturation content at well locations. We used the permeability-porosity relationship shown in Fig. 1.1 as our initial estimate of permeability at well locations. The permeability and porosity profiles from the well were linearly interpolated at inter-wells and extrapolated to create permeability and porosity fields for our reservoir model. We exported the porosity and permeability fields to a commercial flow simulator for production history matching.

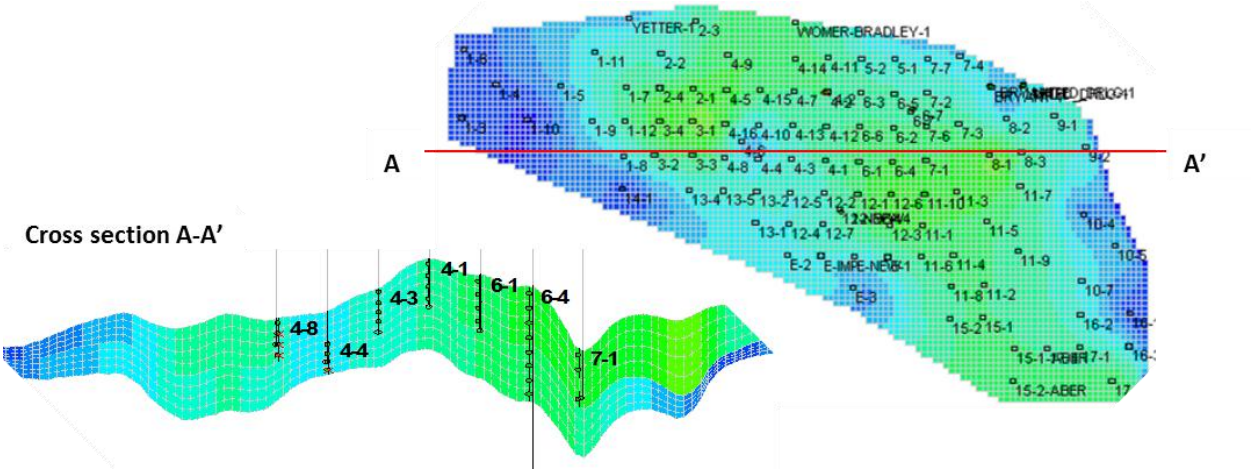

Fig. 1.3 - Simplified model 1 of Ogallah field.

Produced oil and water from well 3-2, well 3-3 in Lease 3, and well 4-12, well 4-13 in Lease 4 were history matched with the field history. The reservoir pressure is stabilized at 1150 psi. Individual well production is evaluated and local adjustments are applied on the reservoir properties around the well area (3 x 3 grid blocks). Table 1.2 shows the summary of the adjusted reservoir properties at the wells in Lease 3 and 4. Although a production history-match appears feasible when modifications on horizontal permeability were made and multiplication factors were applied on the initial water saturation at grid-blocks of the wells, there is no apparent reason, which suggests that the values of the adjusted parameters are similar to the actual reservoir properties. In order to achieve a history match at the well level, the parameters were adjusted as described below:

1. Original porosity values at Well 3-2 and 3-3 were increased by 33%; at well 4-12 and 4-13, the porosity values at the surrounding blocks were increased by 43%.
2. Alterations in porosity and subsequently permeability, caused up to three orders of magnitude permeability difference in adjacent blocks. These alterations modify the values of porosity and permeability beyond the bounds observed from the core data and modern well.
3. Saturation values at the surrounding blocks of well 4-12 and 4-13 were decreased by 43%.
4. Increase the field wise dolomite porosity by 33% and reduce the water saturation of the dolomite interval by 43%.

Fig. 1.5 shows the simulated production of the individual wells 3-2, 3-3, 4-12 and 4-13. In spite of the fairly accurate match obtained at individual wells, the simulated results from the first trial couldn't match the production without heavy adjustment on the petrophysical properties. We further adjusted the field properties following step 4 but the history match results of the simplified reservoir model are very poor as seen in Fig. 1.6.

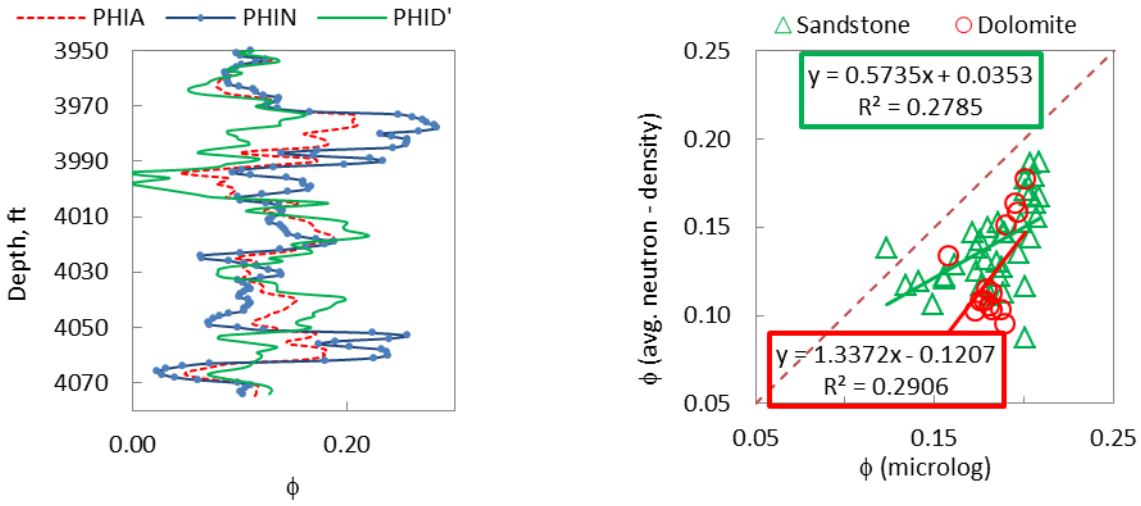

Fig. 1.4 - Transform porosity. (a) Average porosity from neutron-density log of well 4-16; (b) Cross-plot of porosity (microlog) vs. average porosity

Table 1.2 - Adjusted parameters in Lease 3 and 4.					
	Well 3-2		Well 3-3	Well 4-12	Well 4-13
Description	Layer 1	Layer 2	Layer 1	Layer 1	Layer 1
ϕ	0.164	0.201	0.203	0.167	0.196
k (md)	52.94	252.01	258.46	62.52	201.39
Sw	0.382	0.417	0.413	0.427	0.419

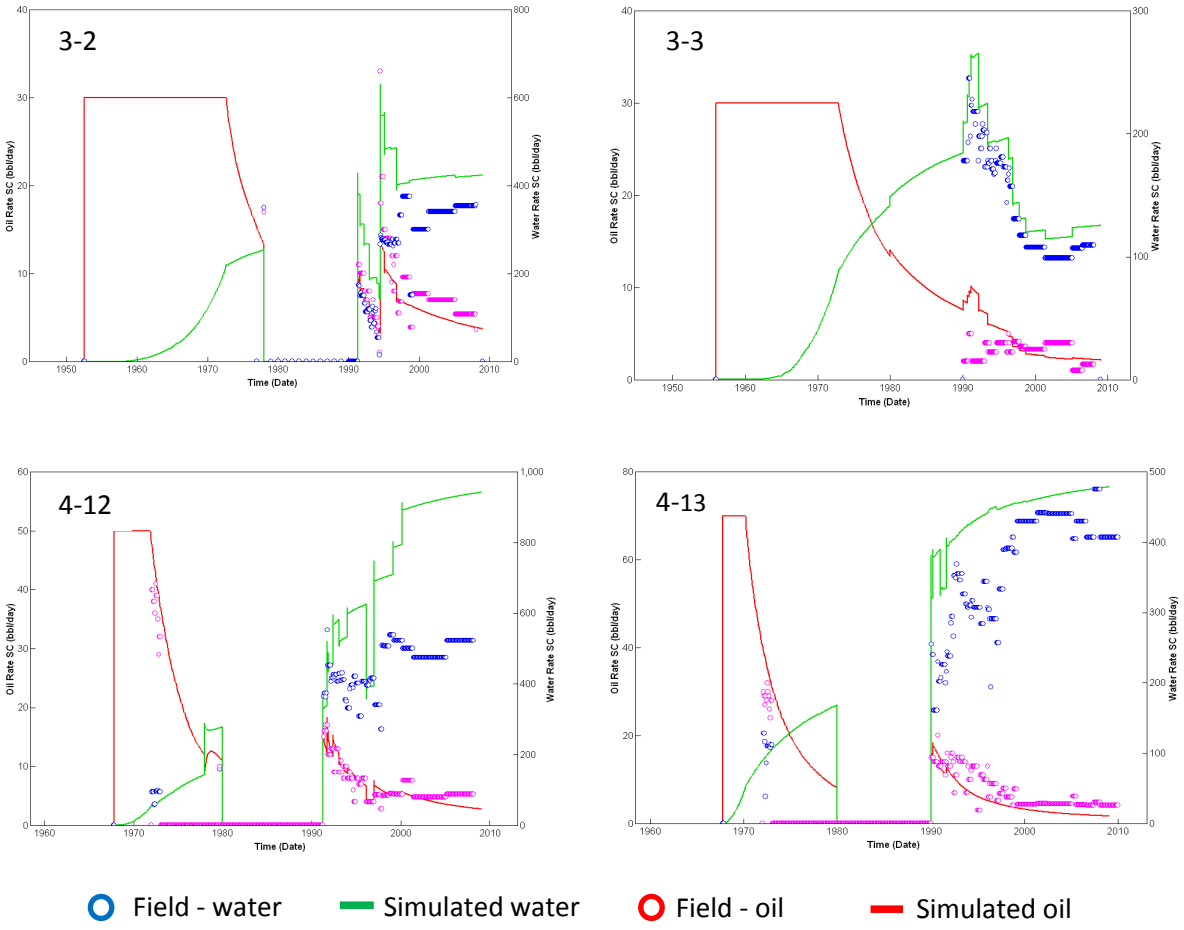

Fig. 1.5 - History match of well 3-2, 3-3, 4-12 and 4-13 from simplified model 1

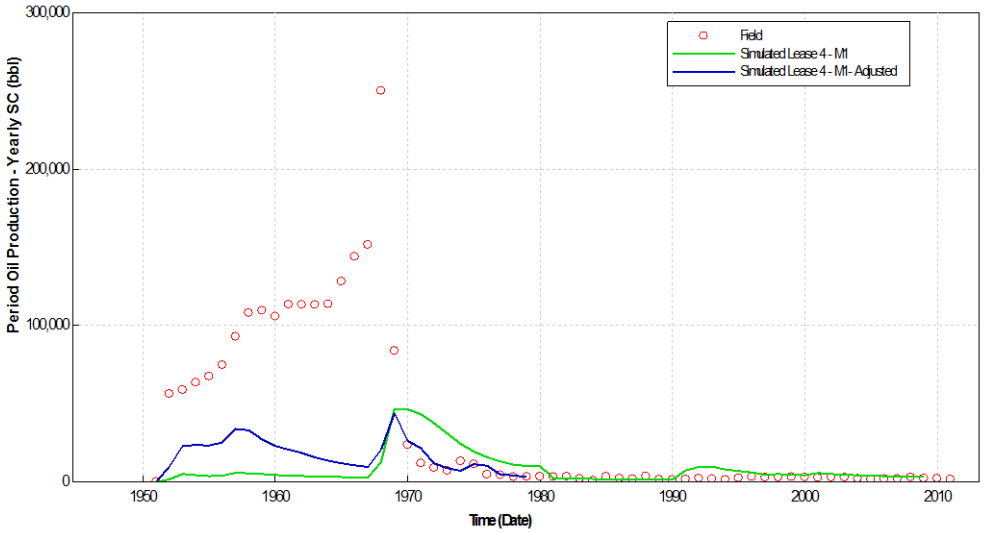

Fig. 1.6 - Lease 4 production from the adjusted and unadjusted simplified model 1.

1.2.2 Second Regression Trial

The first simplified model was modified with the following changes:

1. Microlog resistivities are calibrated against core porosities and applied in each well to determine porosity in the well. A single calibration line is regressed for dolomite based on the spread of the resistivity-porosity data. For sandstone, the resistivity-porosity data was split into two groups, based on the gamma ray measurements, as shown in Fig. 1.7. By inspection, the contact breakpoint is located at GR 35 p.u. reading.
2. The permeability was estimated from logs with an average fit to the porosity-permeability correlations from the core data as shown in Fig. 1.1.
3. The porosity and permeability were averaged along the thickness of each layer and distributed over the field area by least squares interpolation. No geostatistical calculations were used. Structure thickness and depth were added from the core description.

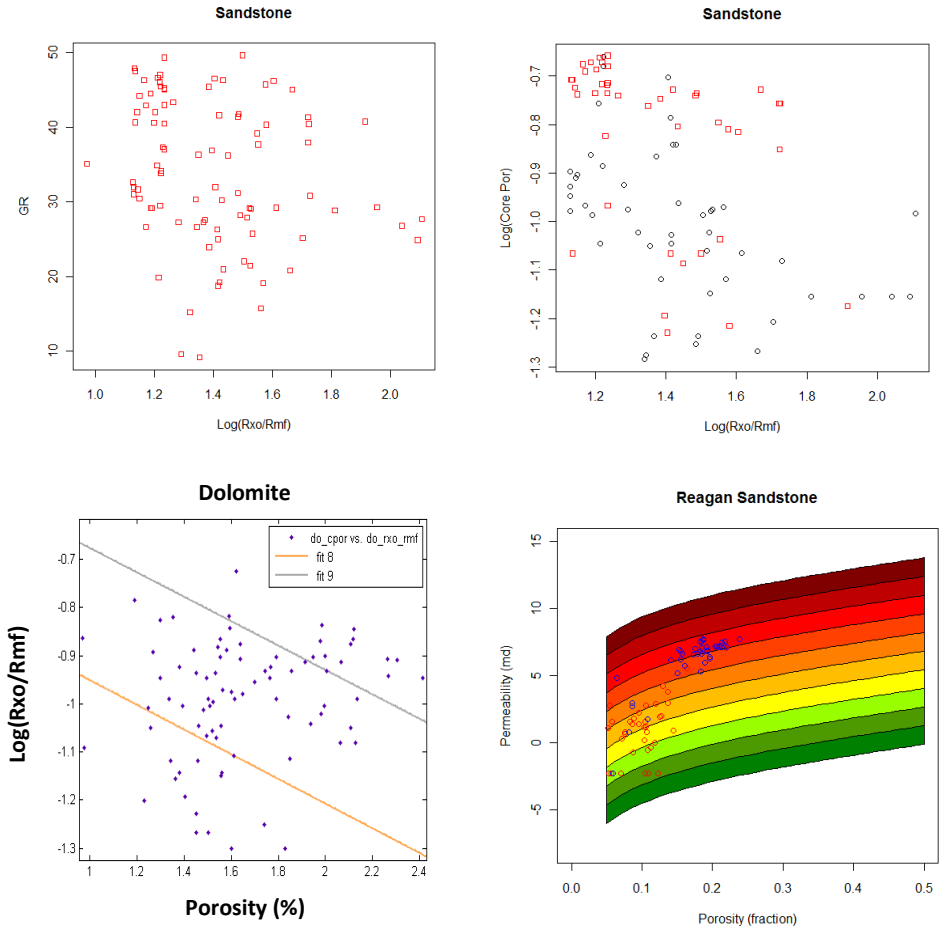

Fig. 1.7 - Porosity transforms using core porosity, Microlog resistivity and GR.

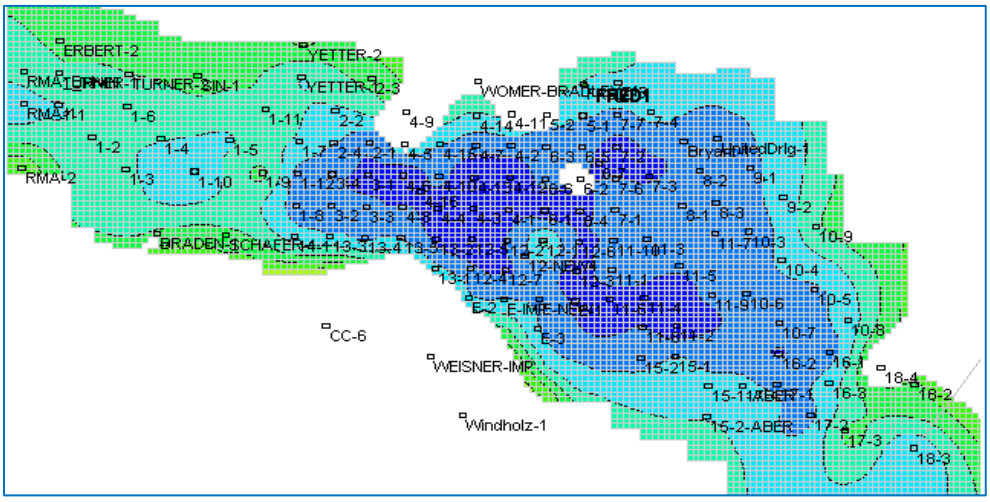

Fig. 1.8 - Simplified model 2 of Ogallah field.

The modified model (2 layers) used in the second trial is shown in Fig. 1.8. Changes made in the reservoir model to simulate the historical performance of the Ogallah field are not sufficient for an accurate history match with the production in leases and in field. As shown in Fig. 1.9, the oil production at Lease 4 is severely under-predicted by the model. Three (3) variables were selected to vary with second regression model:

1. A kv/kh factor of 0.1 was multiplied with the field values of the horizontal permeability to obtain vertical permeability values.
2. Increase horizontal permeability of dolomite intervals by dividing the original values (76 md - 245 md) with a factor of 0.1 and 0.01. The horizontal permeability of sandstone varies from 0.05 md to 2650 md, which is within the range of the expected values, and therefore no adjustment was applied.
3. Altered the end points of relative permeability curves.

In the second simplified model, the field performance of Ogallah was successfully matched after applying a multiplier to the horizontal permeability in the model. This model did not match the leases production history. Simulated WORs of individual wells were compared with the field data but the results were poor. The changes in the second simplified model disregard the continuity of producing formation, and therefore the prediction capacity of the simulation model deteriorated. These significant differences between the simulated results and the actual productions suggest that the model description is inconsistent with the field performance and a more accurate estimate of petrophysical properties is required to match the field production. Simple techniques of modeling the reservoir are not sufficient for such a numerical study. The main drawbacks in the simulation of the first and second model offer a motivation to develop a more geologically consistent model. This has been discussed in the following section.

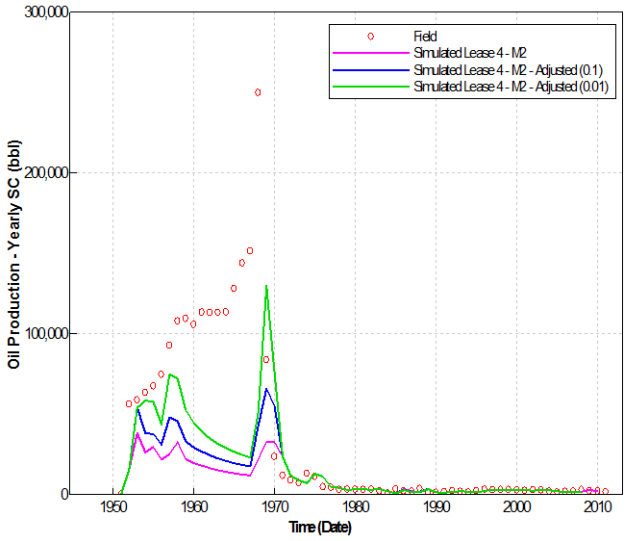

Fig. 1.9 - Lease 4 production from the adjusted and unadjusted simplified model 2.

1.3 Motivations of the Study

The following are the deficiencies in the reservoir models in the initial study:

- The goodness of fit for the defined relationship between neutron-density porosity with microlog porosity to increase the reliability of porosity calculation is poor. Moreover, a geometric average fit (since permeability is on the log scale) under predicts the true mean permeability in the field.
- Petrophysical properties from vintage logs require consistent set of assumptions and interpretation to provide a reasonable volumetric estimate of Ogallah reserves and to build a consistent reservoir model.
- Core plug represents the principal reservoir petrofacies, provides critical permeability estimates for Ogallah reservoir simulation study. Using the generalized permeability-porosity correlation without validation could result in unreliable production simulation. Core analysis or petrophysical data from a rock catalog that represents the reservoir petrofacies would improve the full-field simulation of primary production.
- The lack of consistency in the geological and reservoir simulation model depreciates the hydrocarbon-in-place estimation and the reservoir performance prediction.

Before a model can used for predictive purpose, it is necessary to refine it by first reducing the uncertainty in reservoir properties and then implementing these for a more precise history match. Herein

lies the motivation to construct an integrated reservoir model which addresses the deficiencies in the preliminary models. This thesis addresses the considerations to be taken into account before developing a description of a simulation model based on the availability of data and the heterogeneity of the reservoir. The heterogeneity in reservoir petrophysical properties needs to be quantified in order to reduce their uncertainty. The selection and assignment of rock and fluid properties of the reservoir usually require analysis and interpretation of the data, which best represents the reservoir rock. In the following study, the porosity and permeability distributions of a reservoir have been mostly derived from the core analysis and well logs, while the field performance and other essential source of information (geological studies and drilling reports) are simultaneously considered to ensure that the reservoir properties are appropriately assigned to the model.

1.4 Scope and objective

The scope of the thesis is aimed at four domains of reservoir characterization. (1) The use of core measurements and development of nonparametric correlations to improve porosity and permeability predictions in wells without porosity logs. (2) Application of the nonparametric regression to well logs to estimate petrophysical properties. (3) Population of the petrophysical properties using geostatistical approach for spatial modeling of reservoir properties into a predictive reservoir model. (4) Integration of the field production data into the reservoir model to obtain an accurate history-match.

Chapter 2 summarizes the various aspects of reservoir continuity, petrophysical interpretation and permeability-porosity correlations compiled from the literature. This chapter also reviews the different statistical approaches used to predict the permeability from the well logs and some of the common methods for geostatistical modeling of the spatial properties. Chapter 2 also surveys the common and more recent techniques in history matching. The objectives are to examine the critical parameters that are involved in reservoir characterization, to review the theory of the approaches and to identify the perturbing methods when history matching the reservoir simulation model with the production data.

Chapter 3 illustrates the methodology developed in this research for petrophysical data classification, correlation and prediction using nonparametric regression from well logs. The approach is applied to a heterogeneous reservoir at the Northwestern Kansas: Ogallah field. We compare the results with the core measurements and with the results from the conventional method of obtaining porosity and permeability. We integrate the petrophysical modeling and the nonparametric regression from the well

data into a reservoir description. The objectives are to characterize the reservoir heterogeneity and to integrate information that is known about a reservoir.

Chapter 4 introduces the geology and presents the application of the integrated nonparametric regression for spatial modeling to a heterogeneous reservoir at the Northwestern Kansas: Ogallah field. The details of history matching including the operating conditions and constraints are presented in this chapter. The field example demonstrates the advantages of the improved reservoir description over the conventional approaches in history matching the field production.

We summarized and concluded the results obtained from this thesis in Chapter 5.

CHAPTER 2

LITERATURE REVIEW

2.1 Introduction

The steps in a successful reservoir model include prediction and population of reservoir petrophysical properties and history matching. This literature review chapter presents the methods used to predict porosity and permeability, for populating the reservoir with petrophysical properties, and history matching production data. Sections 2.2 and 2.3 discuss the calculation of porosity from formation resistivity factor using the cementation exponent, *m*. Sections 2.4 and 2.5 discuss the factors that influence the variability in the *m* value and variation in *m* values used in literature. Section 2.6 presents different methods of permeability prediction currently used. Both permeability-porosity relationships as well as permeability prediction from well logs using multivariate statistics are discussed. Different two-point and multi-point geostatistical and simulation techniques used for property population have been discussed in section 2.7. Finally, a review of different history matching methods and their consideration of static and dynamic data is outlined in section 2.8

2.2 Microlog and Core Porosity

The micrologging device is a measuring system where small electrodes measure the resistivity of the formation in the flushed zone that is about 2-3 inches along the length of the well borehole. For zones with no residual hydrocarbon, the formation factor for a clean formation will be equal to the ratio of formation resistivity of the flushed zone, $R_{xo} = R_o$ and the resistivity of the mud filtrate, $R_w = R_{mf}$, which is shown below.

$$F = R_{xo} / R_{mf} \tag{1}$$

The formation resistivity factor, F, is an intrinsic property of a rock related to the efficiency of the paths that conduct electrical current through the medium. The formation factor arises because of the rock porosity and is independent of the electrical conductivity of the fluid in the pores. Archie's law in its original form relates the formation factor to the porosity via the cementation exponent, m, as shown below.

$$F = \phi^{-m} \tag{2}$$

The determination of porosity thus depends upon a knowledge of R_{xo} and R_{mf}. The micrologging measurement responds to the effect of formation that has been flushed with the mud filtrate that displaces the connate water and minimum amount of residual oil saturation is remaining in the pore space (Doll et al., 1952;Smith and Blum, 1954). It has been shown in the literature that deviation of the microlog derived formation factor from core-measured values is governed by the geometric distribution of the conductive fraction in the rock. For a non-shally formation, the formation factor analysis provides the effect of porosity heterogeneity, which can be used to determine porosity of microstructure in the rock. In the invaded zone that is not completely saturated by mud filtrate, the calculated formation factor will be greater than the true value. Since each formation factor corresponds to different poro-space microstructures, the effects of incomplete flushing on different microstructures are distinctive. These effects are accounted for through variation in the m values, using the analysis described in section 3.3.

The microlog information is retrieved from the well log. A good petrophysical interpretation involves developing core and well log interpretations using a calibration model. An intrinsic assumption in the well-core calibration is that the core data is representative of all the uncored elements in the well. Depth matching the R_{xo} from the well log and the porosity from the core involves scaling both the data to the same resolution. Due to fairly regular sampling of the cores from the well, no depth-matching was performed. Development of a log interpretation model without direct calibration can be appropriate provided there is a rigorous integration of rock petrophysics. We applied the methodologies of using core-measured porosity integrated with well log interpreted formation resistivity factor to estimate reliable porosities. We explain the variation of *m* in reference to its relationship with pore geometry based on the classification method – *rfn* for carbonate and FZI for sandstone. The methodology presented categorizes the Arbuckle group reservoir with respect to petrophysical classification of carbonate and sandstone reservoir rocks as an initial step to determine parameters for well log interpretation.

2.3 Choice of Archie Equation for the Model

Various modifications to the Archie equation have been proposed such as Archie-Winsauer, Humble equation, and theoretical derivations of Archie parameters by Haro (2010). The modifications incorporate characteristic values of a and *m* (Humble equation) or allow a variable *m* (Focke and Munn, 1987).

Winsauer et al. (1952) published a generalized form of Archie's equation that has been used in a few studies which is expressed as,

$$F = a\phi^{-m} \tag{3}$$

where *a* is referred to as the tortuosity parameter. Focke and Munn (1987) published another alternative form of Archie equation model for dual porosity expressed as,

$$F = \phi^{-(a+b\phi)} \tag{4}$$

Using a constant *m* value across broad rock types leads to large inaccuracies in petrophysical property determination (Focke and Munn, 1987;Saner et al., 1996;Rezaee et al., 2007;Gomez et al., 2010). Since we characterize the cementation exponent based on the effect of rock fabric and pore throat attributes, we use the original form of Archie equation.

2.4 Parameter m and lithofacies

In a routine formation evaluation, the formation factor and porosity are measured from the core to obtain the *m* parameter for estimating the water saturation. The practice is followed by refining the calculation with the porosity and saturation derived from the well logs. Cementation exponent *m* is usually considered constant for a given rock type. This assumption is not appropriate for a carbonate or sandstone structure that displays complex pore networks and variable particle size, sorting and type of porosity within a single facies.since these attributes significantly influence the *m* values. Focke and Munn (1987) used extensive formation resistivity experiments to demonstrate that more accurate values of *m* can be obtained if a distinction is made between detailed rock types. A single line correlation using Archie's model results in a poor fit to the large data scatter and is unable to capture the variability in the measured resistivity. Using a constant *m* value for a heterogeneous formation will lead either pessimistic or optimistic estimation of water saturation using Archie equation. In our case, the approach will cause inaccurate calculation of porosity using the derived F-ϕ semi empirical equation. While the core could often provide more accurate and precise information about the petrophysical characteristic of a rock unit, the lack of resistivity measurements on cores necessitates the integration of well data into the analysis. The cementation exponent *m* was obtained from the slope of the line representing F-φ relationship in a log-log plot. We derived the formation resistivity factor based on microlog measurements from wells

using Eq. 1. We then determined *m* from Eq. 3 using the porosity from the core samples at the same depth. *m* is determined for each type of lithofacies.

2.5 Cementation exponent or shape factor

The cementation exponent *m* quantifies the electrical conductivity and permeability of a rock by accounting for its pore connectivity. But the cementation exponent *m* is not a constant as it is related to the rock variability in heterogeneous reservoirs. Glover (2009) defines the cementation exponent in terms of the effect of porosity and connectivity on the connectedness of the rock, where the connectedness is the formation conductivity. Therefore, it is clear that the cementation exponent is indicative of the connectivity as well as the porosity of the rock fabric. The cementation exponent is found to exhibit variations within the sample, formation, interval or medium. *m* has been reported to be slightly less than one for fractured rock and up to 3 for compacted sandstone. Salem and Chilingarian (1999) stated that the cementation exponent is highly dependent on the type and shape of the pores and grains as opposed to tortuosity, specific surface area and anisotropy of the rock. Table 2.1 shows the reported *m* value for sandstone.

Table 2.1 - Reported Archie's parameter *m* for the sandstone

Lithology	*m*	Investigator
Unconsolidated sand	1.3	Archie (1942)
Cemented sandstone	1.8 – 2.0	
Clean sand	2.0 – 2.3	Salem and Chilingarian (1999)
Compacted sand	1.8 - 3.0	
Sandstone	1.52 – 2.09	Gomez et al.(2010)

In carbonate, the cementation *m* factor is controlled by the morphology of the porosities which is classified by interparticle and intercrystalline, fracture and separate-vug pore space (Doveton, 2001;Lucia, 2007). Table 2.2 summarizes the *m* values collected by various investigators from the carbonate reservoir. Lucia (1983;2007) provided a range of *m* values from Archie law between 1.8 and 4. Interparticle and

intercrystaline pores which are well connected have a lower *m* value, conversely with the increase isolated pore space that is separate vugs, the *m* value increases (Verwer et al., 2011). On the other hand, touching vug increases the permeability at a given porosity thereby decreases the *m* value (Lucia, 1983).

Table 2.2 - Reported Archie's parameter *m* for the carbonate

Lithology	*m*	Investigator
Non touching vug carbonate	1.8 - 2.9	Lucia (1983;2007)
Wackestone - grainstone	1.775 - 1.926	Saner et al. (1996)
Grainstone (large pores)	2.0 - 2.2	Ramakrishnan et al. (1998)
Fine-packstone-wackestone	1.65-1.70	
Grainstone	1.77	Rezaee et al. (2007)
Packstone	1.84	
Wackestone	2.21	
Bioclast grainstone	1.88	Hasanigiv and Rahimi (2008)
Dolomized packstone -wackestone	2.10	

These extensive laboratory studies show the influences of pore connectivity, grain size,mineralogy and diagenetic and depositional characteristics on the m value in sandstone and carbonate which leads to the presence of many estimation models. Although these models remain attractive in porosity calculation, the associated uncertainty in determining the Archie's m parameters implies that the developed empirical approaches have limited application. Depending on the depositional environment of the formation, quantifying the variation in the cementation exponent based on lithology and pore structures is necessary to obtain accurate estimates of porosity from well logs. When using the reservoir simulator as a predictive tool, it becomes important to predict reservoir parameters accurately, since the errors in their estimates are reflected in the predicted pressures and flow rates from the simulator.

2.6 Permeability estimation and prediction

Along with porosity, permeability distribution is another strong reservoir property that is crucial for an effective reservoir description with large impact on reserves, production forecast and economics of a reservoir. Flow in heterogeneous porous media is mainly controlled by the degree of continuity and connectivity of permeability extremes (Li and Caers, 2011). Therefore, a realistic characterization and representation of channels having the highest contribution to the flow is critical to obtain reliable estimates of production. Permeability is a measurement of rock connectivity to conduct fluid. Archie (1942) indicated that the logarithm of permeability is linearly proportional to porosity and hence the classical approach of obtaining permeability is based on linear regressions or empirical correlations of permeability against porosity. This linear correlation is combined with another between the core-porosities and well log porosities to calculate the permeability at logged well. The method treats any scatter of the regressions as measurement errors and ignores the variations of pore structures in the calculations.

Given a clear petrophysical classifier-separated porosity-permeability relationship suitable for a reservoir, the success of the permeability prediction hinges on the goodness of the implicit relationship between the core-derived petrophysical properties and well log responses. The permeability prediction at uncored wells is largely dependent on statistical methods that may be applied to provide the correlation between the classifier and the well logs responses. For example, Abbaszadeh et al. (1996) presented an improvement in predicting permeability at the uncored wells using hydraulic units (HU) which were estimated using a Bayesian-based probabilistic approach. More recently non-parametric multivariate statistical regression has been applied to overcome the difficulty of developing correlations using well logs for reservoir characterization (Lee et al., 2002;Mathisen et al., 2003a;Perez et al., 2003;Taware et al., 2008). The approach, which is based on regression refinement, has gained wide success in permeability prediction at the uncored wells. Neural networks method is one of the data driven techniques that utilizes log responses to predict permeabilities from logs while accounting for lithofacies (Rogers et al., 1992;Mohaghegh et al., 1997;Soto et al., 2001;Saggaf et al., 2003;Al-anazi and Gates, 2010). Tree-based multivariate and alternating conditional expectations are two other distinctive statistical analyses which have led to accurate estimation of formation permeability in uncored intervals and uncored wells (Perez et al., 2003). These approaches involve clustering well log responses into distinctive classes and improved the correlations of permeability prediction with well logs. Although the method handles the nonlinearity and nonparametric characteristic of the well, the method suffers from the disadvantage of not being able to predict sharp changes in permeability that may be caused because of abrupt changes in depositional environment.

Improvement of the classical method is proposed by first classifying the formation into different lithofacies categories and then regressing linearly the permeability with well logs within these categories. Other researchers include the variability seen in the core by introducing probability field simulations into these linear regressions. Permeability prediction has been performed using permeability-porosity correlations such as the Carman-Kozeny equation and Winland equation, which model the flow channels in rock facies using independent tortuous tubes. The constants in these relationships, however, depend on geological characteristics that are specific to a certain rock group, such as pore geometries, pore throat sizes and rock fabric. There is a causal dependence between the core-derived permeability values and the macroscopic petrophysical attributes, which may have to be log-derived. Therefore, the permeability-porosity correlations have to be developed separately within zones which are characterized by these attributes. For instance, these zones can be classified on the basis of hydraulic units (HUs), which are defined using the flow zone indicator (FZI). They offer improvement over the traditional regression-based averaging method by grouping together the geological and petrophysical properties of rock of similar fluid conductivity at pore scale (Amaefule et al., 1993). The concept of hydraulic units has been used by various researchers to classify porosity-permeability data. For example, Guo et al. (2007) proposed an empirical linear function to transform the FZI into a synthetic rock type and obtained permeability using the porosity-permeability relationship for a given rock type. Corbett and Potter (2004) extended the HU concept to a priori set of global hydraulic elements of a similar petrotype enabling comparisons between reservoirs and to recognize the pattern of the HU for permeability prediction.

In highly heterogeneous carbonates, pore-throat radii area highly variable and difficult to predict spatially, but rock-fabric numbers (*rfn*) tend to be more organized (Lucia et al., 2003). Lucia (1983;1995;2003) proposed using rock fabric type as a classification method to characterize carbonate. This classification model captured the pore structure variability seen on the core scale and permeability is calculated based on the classification method associated with the type of pores for fluid conductivity. While the model is perceived as a conceptual model, the approach is based upon global-default parameters which are applicable to obtain permeability for various carbonate reservoirs.

2.7 Spatial modeling

The spatial distribution of hydrogeologic reservoir properties like porosity, permeability and facies across the reservoir is critical towards a successful simulation and accurate history match. Modern geostatistics

aims at building an algorithm that simulates the data distribution of the unknown variables and generates alternative outcomes based on the inherent uncertainty in the variable. The approaches to populate the reservoir properties can be broadly classified into 2-point/multipoint statistical approaches utilizing variograms/kriging and simulations. Variograms model the spatial covariance of the petrophysical properties across the extent of the reservoir. Cross-variograms can be used to model the distribution simultaneously for different data types (Goovaerts, 1997, Chiles and Delfiner, 1999, Journel and Huijbregts, 1978 and Wackernagel, 1995). In order to populate unknown data and account for over-sampling at specific locations, kriging (Krige, 1951, Matheron, 1970, Journel and Huijbregts, 1978) is performed. Kriging consists of producing an independent and orthogonal basis for the original data and then a linear regression through this with the weights obtained by minimization of the error variance. The matrix of weights is based on the variogram. Different types of kriging are used such as ordinary kriging, co-kriging, indicator kriging can be used along with the corresponding variograms. They offer advantages such simultaneous modeling of different data types in cokriging and location-specific prior probability for indicator kriging. Using a simple variogram and kriging method gives an estimate of the mean and variance of the properties in a reservoir. However, to produce realizations that retain specific features and heterogeneity in the reservoir, various covariance-based stochastic simulation algorithms are used. Broadly, these are based on a Gaussian random function or on a indicator expected simulation. The random function gives the cumulative probability density of the property at a spatial location under the condition of the available data. An example is the sequential simulation algorithm (Deutsch and Journel, 1998, Goovaerts, 1997, Chiles and Delfiner, 1999 and Rosenblatt, 1952). Approaches for sequential simulation include both two-point statistical methods (variogram) (Goovaerts, 1997 Anderson, 2003, Chiles and Delfiner, 1999 and Gomez-Hernandez and Journel, 1993) and multi-point approaches such as training images (Guardiano and Srivastava, 1993, Srivastava, 1994, Strebelle, 2000,2002, Zhang et al, 2006). Object-based algorithms have the advantage of being able to reproduce spatial structures and patterns in the reservoir, while multi-point or pixel-based algorithms have the advantage of being easily conditioned. Some two-point simulation algorithms include sequential Gaussian simulation (Journel 1993; Goovaerts, 1997), direct sequential simulation (Journel, 1994; Bourgault, 1997), direct error simulation (Luenberger, 1969; Journel and Huijbregts, 1978; Chiles and Delfiner, 1999), indicator simulation (Journel, 1983, Goovaerts, 1997; Chiles and Delfiner, 1999).

Modern variations of sequential Gaussian simulation include features such as cokriging, collocated cokriging with the intrinsic model, and cokriging with a linear model of coregionalization for the cosimulation of multiple variables, incorporation of multiple secondary data using locally varying means, collocated cokriging, and Bayesian updating (Manchuk et al, 2011). Multiple-point simulation

algorithms (Remy et al., 2009) include the single normal equation simulation (Guardiano and Srivastave, 1993; Strebelle, 2002), filter-based algorithm (Arpat, 2004; Zhang, 2006; Journel and Zhang, 2006) and hierarchical simulation (Maharaja, 2004). Different simulation algorithms can lead to differences in spatial distribution of properties (Alabert et al, 1992;Gomez-Hernandez and Wen, 1998; Gotway and Rutherford, 1994; Journel and Alabert, 1989; Scheibe and Murray, 1998; Western et al, 2001; Zinn and Harvey, 2003). Lee et al (2007) conclude from an observation of the drawdown response and the numerical simulation of the reservoir that an ideal model for reservoir population should account both for the facies structure as well as the random variation in properties within each facies. They also stress that indicator based modeling, such as transition probability-based geostatistical simulation (TPROGS) is essential in systems of distinct facies, since it facilitates more hydraulically connected networks and stronger spatial continuity in a high-K system. The Gaussian model, on the other hand might miss important geologic characteristics even if it is exhaustively determined and closely fits the exponential function. Ensemble Kalman filter (EnkF) (Evensen et al, 2007) is an algorithm which provides real-time updating and prediction in reservoir simulation models. The analyzed system provides optimal realizations of the reservoir properties which are conditioned on all previous production data. EnkF is suitable for parameter estimation in cases with a large number of poorly known parameters. A number of combinations and variations of the above methods with incorporation of lithofacies classes, parallel processing and multi-point approaches exist. Almeida (2010) analyzed truncated gaussian simulation, posterior conditioning and classification of simulated probabilities based on local and global proportions (TGSPC), TGSPC+Simulated Annealing (SA), Sequential indicator simulation (SIS), SIS+SA and probability field simulation (PFS). The preferred method of modeling the geology depends on the reservoir, but SIS is the most commonly used method.

2.8 History matching

History matching consists of integrating production and pressure history data (dynamic data) into the reservoir model during the development and management of the petroleum reservoirs. Matched models are necessary to ensure reliable production forecasts and to increase the understanding of the geological and reservoir models. An adequate match to the field data is difficult because the relationship between the reservoir properties and the dynamic data is highly nonlinear and therefore the history-matched solutions are non-unique (Caers, 2003;Schiozer et al., 2005;Hoffman et al., 2006). Generally, the goal of history matching is to produce a history match and a predictive reservoir model. In the common practice of history matching, geoscientists provide an initial model and reservoir engineers perturb the reservoir

properties until the history productions are matched. The history matching is often done with a trial-and-error method. The attempts of honoring these dynamic data ends up with unrealistic history-matched models from a geological and geophysical point of view or a single matched model which provides very little information about reservoir uncertainties.

To improve a reservoir model, Hoffman et al. (2005;2006) proposed the probability perturbation method (PPM) that integrates all source data to create a history-matched reservoir model while maintaining the conceptual geologic model. Other methods to integrate production and geosciences data include, multiple point (MP) geostatistic with training geological images to infer spatial properties (Caers, 2003), multi-scale history match using block Kriging with sequential Gaussian simulation (BKSGS) (Aanonsen, 2008), and uncertainty analysis that history-matched models are generated and the unfit models are discarded when incorporating dynamic data (Schiozer et al., 2005). However, the application of these routine methods has been limited to practical consideration in real field cases. Reservoir flow-unit characterization technique has been attractive for generating an accurate permeability estimate. The methodology has been confirmed by successful history match without permeability modification in the field (Guo et al., 2007;Shenawi et al., 2007;Bhattacharya et al., 2008;Rahmawan et al., 2009).

2.9 Summary

The chapter presented a literature review of the existing methods of petrophysical property estimation, spatial population of properties, and some aspects of history matching. The cementation exponent used to calculate porosity depends on the pore characteristics, mineralogy, grain size, connectivity, presence of vugs and various other diagenetic and depositional characteristics of the rock. Various m values for sandstone and carbonate used in literature were presented. Current practices of estimating permeability which discuss aspects of permeability-porosity correlations as well as permeability prediction from well are presented in this study. The basic concepts of flow-unit and HU classification and their application in developing permeability-porosity relationships from cored information were reviewed. The sections discussed the statistical techniques used to correlating the cored HU or permeability information to the logged wells. The influence of pore connectivity and lithofacies on the porosity-permeability relationships is clear from the literature review.

Current geostatistical methods in literature used to perform petrophysical property population were then reviewed. The spatial variance is described using variograms and can be interpolated using

various forms of kriging. Multiple-point algorithms used to populate data and current methods of property simulation were also briefly reviewed. History matching and current techniques used for history matching, some of which simultaneously honor geological and dynamic data are briefly discussed. Based on the literature review, the objectives of the methodology to be developed are as follows:

1. To develop a method of rock classification based on pore characteristics that influence connectivity.
2. To separate the well logs into distinct lithofacies group so that petrophysical property analysis can be performed individually in each group.
3. To develop a strategy to simulate the petrophysical property population in the reservoir. To develop a methodology for simulation which can history match the dynamic production data, while honoring the geological information.

CHAPTER 3

METHODOLOGIES

3.1 Introduction

This chapter presents the characterization of the reservoir rock based on core data and the methodology to obtain the porosity and permeability using integrated well logs and core data. An intrinsic assumption is that the core measurements are representative of the petrophysical interpretation in the entire formation. Sections 3.2 and 3.3 discuss about classification of the core petrophysical properties based on lithology and pore space attributes of the rock. These classifiers are rock fabric numbers for the carbonate and FZI for sandstone. Section 3.4 discusses the collective response of the well logs and their corresponding lithofacies developed as electrofacies for the reservoir. Sections 3.5, 3.6 and 3.7 present the multivariate statistical analyses involves in classifying the well logs based on lithofacies data. The clusters are used as priors for model based discriminant analysis, which is used to predict the clusters using well logs. Section 3.8 discuss the transform models for well logs and predictors that have been determined from the carbonate and sandstone clusters obtained. The representative transforms are then used to predict the porosity and permeability. In section 3.9 we demonstrate the field application of the proposed methodologies. A comparison of the core petrophysical properties with the predictions based on the zoning criteria shows a strong goodness of fit. An understanding and incorporation of this methodology is expected to improve results in reservoir characterization.

3.2 Samples Classification

Various authors have developed transforms specific to carbonate rocks, primarily utilizing information on the rock structure, pore types and lithology. Lucia et al. (2003) proposed a continuum of petrophysical classes called rock-fabric numbers (*rfn*) based on grain size, crystalline structure, sorting and type of pore space. He used a visual description of carbonate pore space to classify porosity permeability relationships. He estimated Archie's exponent *m* and capillarity based on the pore space description with particular focus on touching and separate vugs. Amaefule et al. (1993) proposed a method of petrophysical relationship zoning based on the flow zone indicator (FZI).

The rock fabric number, proposed by Lucia (1983), is a suitable parameter that characterizes the interparticle pore size distribution of the Arcbuckle rock. Byrnes et al. (1999) studied the core samples

from the Arbuckle reservoirs in Kansas and obtained a petrophysical trend of the Arbuckle carbonate properties. An overlay of Byrne's lithology study for the Arbuckle carbonate with Lucia's *rfn* based classifiers on the same porosity-permeability cross-plot shows that each lithology identified by Byrnes falls within a specific *rfn* range. Byrnes data includes a comprehensive span of lithologies ranging from homogeneous medium-grained ooid packstone-grainstone to finer grained mudstone. There exists a correspondence between the lithological description and the *rfn*, however, it is noted that the *rfn* does not explain all the aspects of the lithology which could have an effect on the cementation factor. A limitation of the *rfn* classification may be its non-applicability in the presence of touching vugs. However, a majority of the Arbuckle carbonate core samples lie within the range of applicability stated by Lucia.

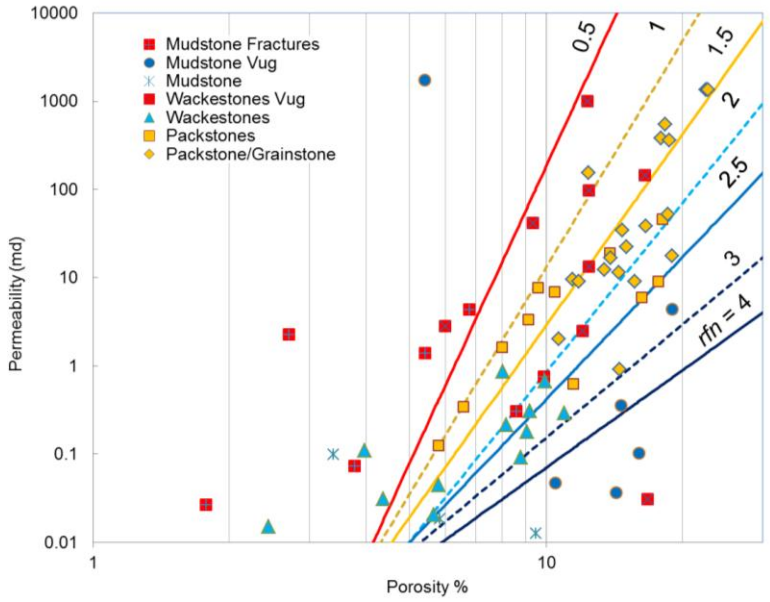

Fig. 3.1 - Permeability vs. porosity cross-plot of Arbuckle group core-plug (Steinhauff et al., 1998; Byrnes et al., 1999) overlay with rock fabric classification (Lucia, 1983).

Sandstone has been classified based on grain size, packing and sorting, and the cementation exponent of the rock. In general, the cementation exponent has been found to have an inverse relationship with the permeability of sandstone. Frailey et al. (2011) used groupings of Archie's sandstone *m* to separate the porosity-permeability plot into zones characteristic of *m*. Inter-relationships have been developed between permeability, porosity, formation factor and parameters like tortuosity, which are representative of the pore structure of sandstone. The porosity in sandstone has been found to have an exponentially decreasing trend with depth (Frailey et al., 2011;Medina et al., 2011), which could be attributed to the effects of compaction and overburden pressure. A classification of sandstone petrophysical relationships

using FZI was published by Amaefule et al. (1993). The FZI method was validated by characterizing clastic and carbonate reservoirs from different regions.

3.3 Petrophysical Classifiers

Carbonate petrophysical classification from Lucia transforms the core description of the Arbuckle dolomite to rock fabric number. The rock fabric numbers *rfn* are the geological descriptors that characterize the pore according to particle size and sorting, interparticle porosity, and various types of vuggy porosity. Lucia defines *rfn* as follows,

$$Log(k) = [A - B\log(rfn)] + [(C - D\log(rfn))Log(\phi)] \quad (5)$$

where A = 9.7982, B = 12.0838, C=8.6711, D=8.2965. The theoretical concept behind the classification is that the interparticle pores that are well-connected result in good conductivity for the flow of the electric current. The corresponding *rfn* value decreases with increasing grain size. The cementation exponent *m* indicates the resistivity, or conductivity variation at a constant porosity because of the pore connectivity of the rock. A sample with a poor electrical conductivity will result in higher resistivity thereby increasing the *m* value. This notion suggests that well-connected interparticle porosity will have both lower *m* and *rfn* value. For a rock with separate-vug porosity, *rfn* value will increase due to isolated pores that do not contribute to flow, which also corresponds to the concept of *m* value in the Archie model. Thus, the *rfn* and the cementation exponent of the rock fabric display similar trends with respect to the pore-size distribution and interconnection of the rock. For the Arbuckle dolomite, *rfn* values are computed from the core measurements of permeability and porosity using Eqn. 5. The data are grouped into four categories – 0, 1, 2 and 3 according to the range of *rfn*. For each category, the mean *rfn* and mean *m* value are regressed to develop a suitable correlation as shown in for Arbuckle dolomite.

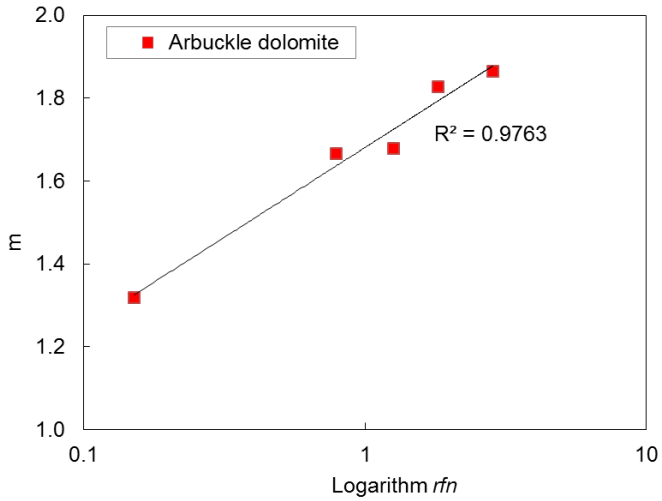

Fig. 3.2 - *m* vs. *rfn* of the Arbuckle dolomite core samples from the Ogallah.

Overall, it has been observed that some of the variation in cementation exponent of sandstones can be explained based on porosity and permeability of the rock. The flow zone index (FZI) is an indicator of the sandstone grain size, shape, sorting, tortuosity and other properties that are indicative of flow path. FZI relationship derived from Kozeny-Carman's relationship as shown in Eqn. 6 was published by Amaefule et al. (1993).

$$FZI = 0.0341\sqrt{k/\phi^3}(1-\phi) \tag{6}$$

The approach was initially proposed to improve the porosity and permeability correlation for a given rock type. Amaefule et al. (1993) designated FZI as a unique parameter that varies inversely with tortuosity, shape factor and grain surface area, which are the critical factors determining the flow in the rock. The FZI value classifies the pore geometry as flow zones where a high FZI value indicates that the rock exhibits coarse, well-sorted grains and lower shape factor. In the same manner, a low FZI value represents a rock which has fine and poorly sorted grains. The cementation exponent accounts for the effect of porosity and of the connectivity (inverse of tortuosity) of the pores on the connectedness of the rock, and thus on the flow properties of the sandstone. Glover (2009) defines the cementation exponent in terms of connectedness, G, that is the inverse of formation resistivity as shown in Eqn. 7.

$$m\chi = dG/d\phi \tag{7}$$

where χ is the connectivity of the rock matrix. The connectivity is the reciprocal of tortuosity. There is a strong correlation between the FZI value and the cementation exponent, which is driven by the attributes

of grain interconnectivity, texture and mineralogy of the rock. In the Ogallah, the sandstone petrophysical data is grouped into ranges of FZI values. The average *m* values were calculated for each FZI range by fitting the original form of Archie equation to the corresponding formation resistivity versus porosity data. Based on the obtained cementation exponents, a correlation, as shown in Fig. 3.3, was developed between the mean FZI and mean *m* in each FZI range.

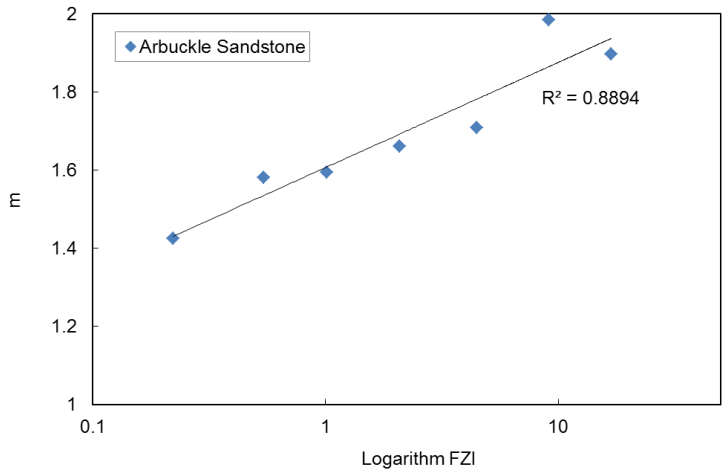

Fig. 3.3 - - *m* vs. FZI of the Arbuckle sandstone core samples.

Linear relationships observed between the petrophysical classifiers *rfn*/FZI and the average cementation exponents show that when the *m* values within a specific classifier range, but representing various different facies were averaged, the cementation exponent and petrophysical classifier show a clear correlation, proving that they explain similar pore throat attributes. The next step was to extract the cementation exponents out of well log data, so as to estimate porosities in uncored wells. For this purpose, the well log data were first separated into groups, and *m*-well-log correlations were developed within each group, where each group was proved to correspond to a specific lithofacies from the core description. This way, the variations in m-value were attributed to change in the pore connectivity and porosity variations, since the variation in lithofacies within each well log group was kept to a minimum. The effect of incomplete flushing is also accounted for via variations in the m value within a specific lithofacies. Since the extent of incomplete flushing is dependent on the lithofacies, this procedure can be justified. It has been demonstrated that the cementation exponent and the petrophysical classifiers represent similar attributes of the rock namely pore-size distribution and connectivity; nevertheless these parameters do not overlap entirely in their representation of the rock structure; therefore, the transforms for the cementation exponent and the classifiers are developed independently.

3.4 Electrofacies and Petrophysical Prediction

The conventional approach of estimating petrophysical properties from the well logs assumes that the petrophysical properties can be obtained from the well logs using some preconceived models. However, these approaches are likely to be less predictive when the pore characteristics of the lithology are dominating factor of the petrophysical properties. To attain more representative petrophysical properties from well logs, we perform multivariate data analyses to correlate well log responses with the petrophysical properties measured from the core. A multivariate data analysis involves clustering the well-log responses with similar characteristics into electrofacies and is expected to lead to an improved petrophysical properties estimation using well logs. Serra and Abbott (1982) developed the concept of electrofacies from well logs and extended the petrophysical properties identified from the core to the well logs. The authors defined electrofacies as collective well logs responses that represents the facies uniquely because well logs measurements are a function of facies characteristics and properties of the rock. Numerous reservoirs illustrate the importance of electrofacies characterization for permeability estimation from well logs and improved reservoir characterization using different computing techniques (Bucheb and Evans, 1994; Lim et al., 1997;Lee et al., 2002;Mathisen et al., 2003;Perez et al., 2003;Taware et al., 2008). The log responses represents many characteristics of a rock for example, a resistivity log corresponds to the type of formation fluid, porosity, degree of cementation, tortuosity, and amount of shale, while a gamma ray is indicative of radioactivity chemical content in the rock. Principal component analysis (PCA) was used to transform well logs to scores and model-based clustering was used to categorize the scores into electrofacies groups. These steps utilize the pattern of information contained in well log measurements to arrive at an insightful classification. We utilize alternating conditional expectations algorithm to determine the petrophysical correlations from well log measurements within the clusters.

3.5 Principal Component Analysis

The principal component analysis (PCA) form of mathematical application is to reduce the dimensionality of a diverse dataset and provides the optimal representation of the data. PCA transforms the original variables with the principal components and reorders the principal components according to their contribution to the variance in the original variables. To apply the principal component analysis in the formation observation, consider a suite of well log responses $X_{m\times n}$ of *m* types with *n* depths in which the

element x_{ij} is the reading of the $j=(1,\ldots,m)$ well logs at depth $i=(1,\ldots,n)$. The covariance of the matrix is given as,

$$C_x = \frac{1}{n} XX^T \tag{8}$$

An eigenvalue decomposition of the covariance matrix, shown in Eqn. 4, is performed to express the covariance matrix in terms of the matrices of eigenvalues and eigenvectors. The diagonal matrix D contains the eigenvalues corresponding to each of the eigenvectors.

$$C_x = EDE^T \tag{9}$$

Each resulting eigenvector contains a part of the total variability and is uncorrelated to those from other eigenvectors. The eigenvalue corresponding to each eigenvector is the variance contained along each eigenvector. The principal components, **P**, of the well logs are given by the product of the transpose of eigenvector matrix, **E**, and **X**,

$$P = E^T X \tag{10}$$

The principal components are an alternative form of representing the well logs, with the advantage that there is no correlation between the information represented by each of them. Further, since a majority of the variance in the data is contained in the first few components, any noise in the data can be separated. PCA extracts the uncorrelated descriptors from the well logs measurement in the form of principal components, thus the principal components are linearly independent and describe the dataset concisely for further multivariate analysis. The limitation to developing correlations against the principal components as opposed to the well logs themselves is that it is difficult to pinpoint the physical meaning of the principal components, and their relationship with fundamental pore structure properties. Fig. 3.4 shows the scatter plot of the principal components of the well logs with cores and the principal components generated from the well logs with no core for dolomite and sandstone formations from the Ogallah field. From the range of the principal components which had corresponding cores from 18 wells, the PCA analysis is shown sufficient to explain the variations seen for the whole field.

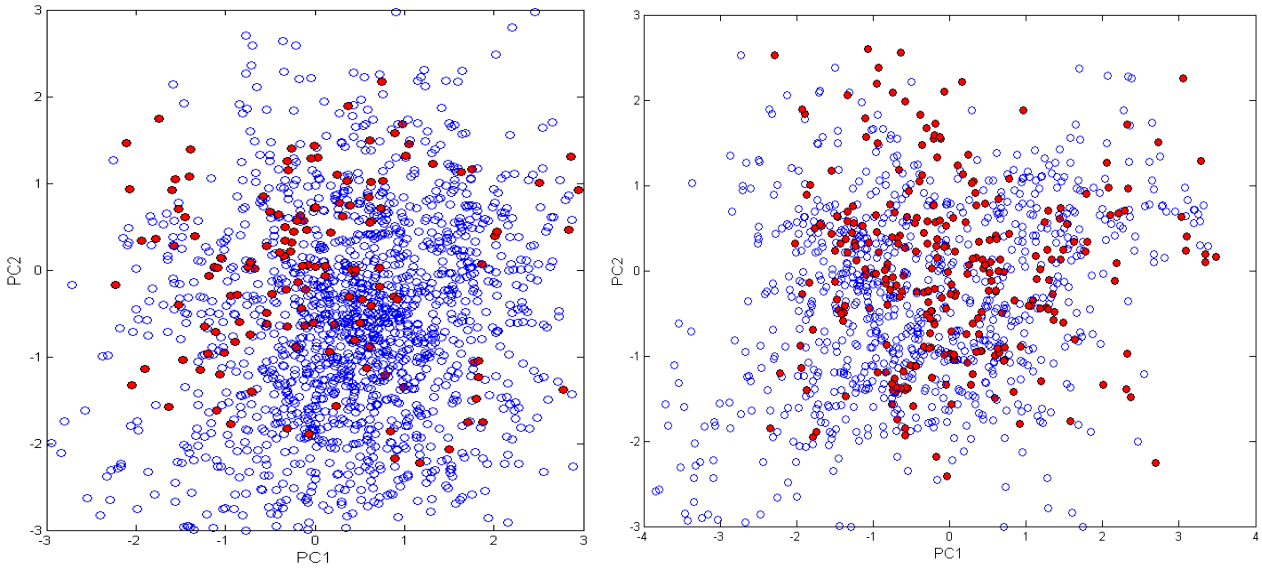

(a) Dolomite **(b) Sandstone**

Fig. 3.4 - Scatter plot of PC1 vs. PC2 from the core and uncored wells. Filled circles in red represent cored data; Blue circle represent uncored data.

3.6 Clustering Analysis

Clustering analysis is used to group the dataset into clusters that are internally homogeneous because of similarity within the cluster, but externally isolated due to dissimilarity between the clusters. The purpose of the clustering analysis is to well-separate the groups from a dataset into meaningful groupings. In traditional approaches to clustering, the underlying algorithm criterion is without an association with the statistical models therefore these methods do not perform well in instances where the clusters are not well separated or when the number of clusters is unknown. Finite probability mixture models for clustering are considered to be very general and quantify the applicability of a clustering method. Using these models, the clustering is performed by maximizing the likelihood of the model given the data. The classical clustering methods, like K-means clustering method, are a case of model-based clustering as when the covariance matrix is the same for each component and proportional to the identity matrix. In this section, we summarize a strategy of the clustering analysis based on mixture models (Fraley and Raftery, 2002); to separate the well logs data into electrofacies. The mixture models assume that each cluster of the data is generated by an underlying probability distribution. Supposing the data $\boldsymbol{x}$ consist of

independent multivariate observations $x_1,\ldots,x_n$ and G is the number of the clusters in the data. The likelihood for the mixture model is

$$L_{mix}(\theta_1,\ldots,\theta_1|x)=\prod_{i=1}^{n}\sum_{k=1}^{G}\tau_k\phi(x_i|\theta_k) \tag{11}$$

Where τ_k is the probability that an observation comes from k th cluster and θ_k is the parameters of the kth cluster. The observations are viewed as coming from the mixture density function of each cluster, $f(x_i)$, given as eqn. 12.

$$f(x_i|\theta_k)=\sum_{k=1}^{G}\tau_k\phi(x_i|\mu_k,\Sigma_k) \tag{12}$$

The mixture density function is represented by Gaussian mixture models as seen in Eqn. 13. In the Gaussian mixture model, each of the clusters is modeled by the multivariate normal distribution with mean vectors, μ_k and the covariance matrix, Σ_k

$$\phi(x_i|\mu_k,\Sigma_k)=\frac{\exp\left\{\left(-\frac{1}{2}(x_i-\mu_k)^{\mathrm{T}}\Sigma_k^{-1}(x_i-\mu_k)\right)\right\}}{2\pi^{\frac{k}{2}}|\Sigma_k|^{\frac{1}{2}}} \tag{13}$$

The covariance matrix, Σ_k determine the geometric features such as the orientation, size and shape of the k th cluster. The structure of the covariance matrix was further represented in terms of its' eigenvalue decomposition.

$$\Sigma_k=\lambda_k D_k A_k D_k^T \tag{14}$$

where D_k is the orthogonal matrix of eigenvectors, A_k is a diagonal matrix whose elements are proportional to the eigenvalues, and λ_k is the associated constant of proportionality. The matrix D_k determines the orientation of the component, A_k determines its shape and λ_k determines its volume. The model based clustering method has the advantage of model selection properties, which fit for different scenarios arising from the data. In addition, the Bayesian information criterion (BIC) algorithm within the model-based clustering probabilistic framework allows the issues of choosing the best

clustering algorithm and the correct number of clusters to a model selection problem. The classification likelihood of the mixture model is estimated using expectation-maximization (EM) algorithm (Fraley and Raftery, 2002). The EM algorithm alternates between a maximization step where the parameters of the distributions are recalculated, using eqn. 14-a, and an expectation step, where the clusters are reassigned.

$$\hat{z}_{ik} = \frac{\tau_k f_k\left(x_i \mid \theta_k\right)}{\sum_{j=1}^{G} \tau_j f_i\left(x_i \mid \theta_j\right)} \tag{14-a}$$

The values of $\hat{z}_{ik}$ that maximize the log-likelihood defined in Eqn. 14-a define the estimated conditional probability of belonging to group k for every observation x_i.

$$l = \sum_{i=1}^{n} \sum_{k=1}^{G} z_{ik} \log\left[\tau_k f_k\left(x_i \mid \theta_k\right)\right] \tag{14-b}$$

The BIC ensures that the number of clusters required to maximize the likelihood of the data is kept to a minimum. Fig. 3.5 shows the scatter plot of PC1 and PC2 divided into their electrofacies based on the unique characteristics of the well log measurements. The identified clusters are calibrated with the core observations to ensure their interpretable petrophysical meaning.

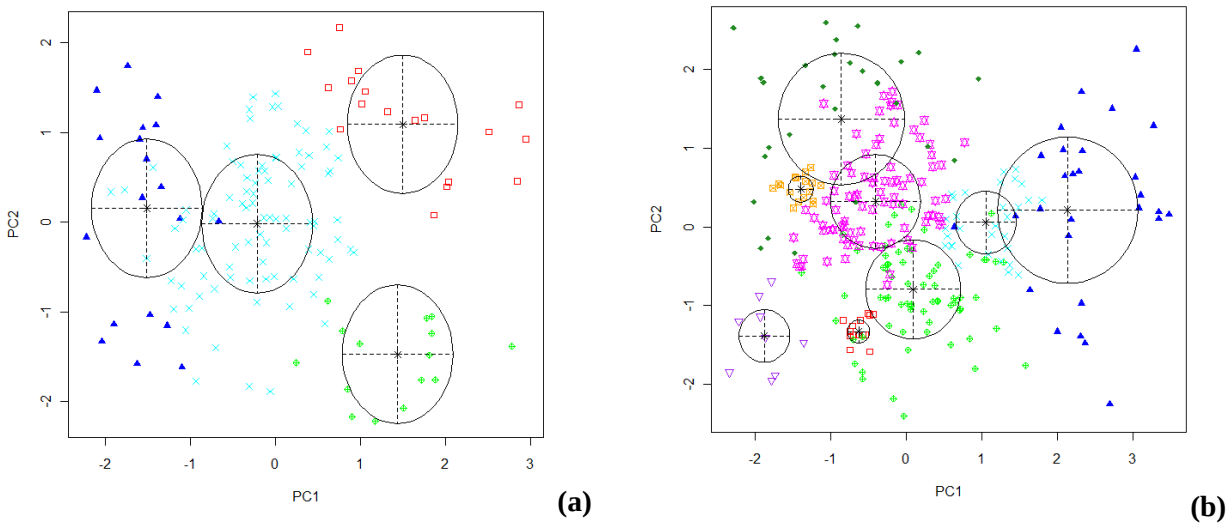

Fig. 3.5 - Scatter plot of PC1 and PC2 showing the identified electrofacies for (a) Arbuckle dolomite and (b) Reagan sandstone.

The clustering algorithm indicates that four (4) distinct electrofacies groups were identified from the well log measurements of the carbonate interval and eight (8) electrofacies groups were identified for the sandstone intervals. A qualitative investigation of the clusters was further confirmed by comparison of the clusters with the lithofacies described in the core analysis as shown in Fig. 3.6. It can be seen that the number of electrofacies groups predicted by model-based clustering agreed well with the lithofacies groups interpreted from the core analysis. For example, in the case of dolomite, we may match cluster 1 with crystalline dolomite, cluster 2 with sandy and argillaceous dolomite, cluster 3 with limy dolomite and cluster 4 with vuggy dolomite. Thus, the result of the predicted electrofacies agrees well with the core data.

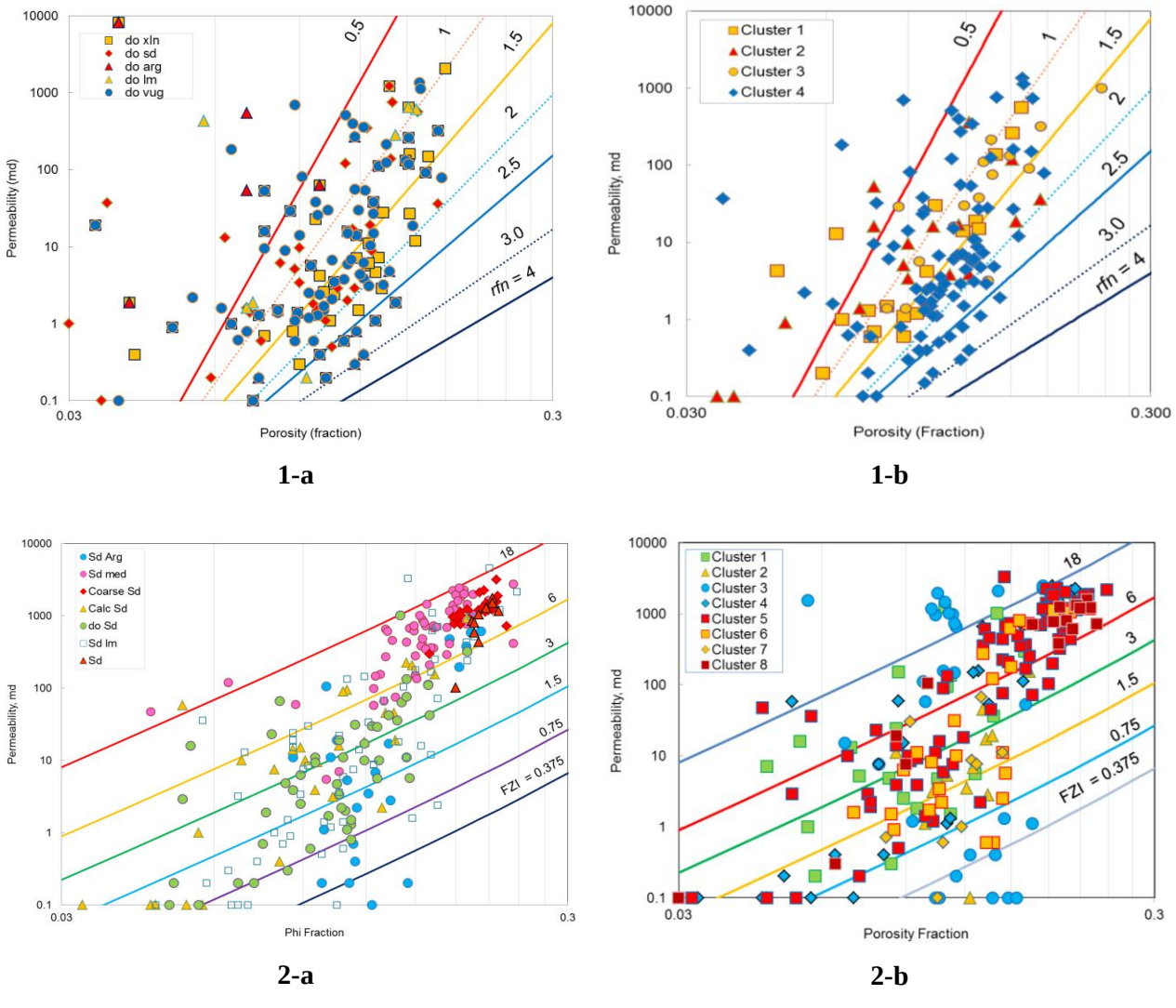

1-a **1-b**

2-a **2-b**

Fig. 3.6 - The identified electrofacies and lithofacies from core.

3.7 Discriminant Analysis

Discriminant analysis is a supervised classification method that seeks a rule that will allow the prediction of the cluster to which the observation may belong. The aim of the analysis is to use the known classification of some observations generated by probability distribution, to classify others. In a discriminant analysis, the observations ***x*** in cluster ***k*** are assumed to be multivariate normal is represented with a single Gaussian density model, $f_k(x)$, is given in Eqn. 13. According to the Bayesian classification rule, the observations ***x*** is assigned to the cluster to which it has the highest posterior probability of belonging. And if τ_{jk} is the proportion of members of the populations that are in cluster ***k,*** the Bayes' theorem says that the posterior probability that an observation ***x*** belongs to cluster ***k*** is expressed as Eqn. 16.

$$\Pr[x \in class\ j] = \frac{\tau_j f_j(x)}{\sum_{k=1}^{G} \tau_k f_k(x)} \tag{16}$$

In a linear discriminant analysis (LDA), the covariance matrices for the different clusters are the same (e.g. $\sum = \sum_k$ for $k = 1,\ldots, G$) for all classes and therefore the decision boundary between the groups is linear . An alternative approach to generalized LDA, which has gained popularity, is to allow the density for each cluster itself to be a mixture of normal. In a discriminant analysis based on EM, the observations ***x*** in cluster ***k*** are assumed to be multivariate normal and represented with a Gaussian density model, $f_k(x)$ for each group k, as shown in Eqn. 17. As in model based clustering, the parameters of the model, θ_k and the mixing proportions τ_k are obtained by the EM algorithm, while maximizing the conditional probability of group assignments for all observations.

$$f_j(x|\theta_k) = \sum_{k=1}^{G} \tau_{jk} \phi(x|\mu_k, \Sigma_k) \tag{17}$$

The concept of the model-based discriminant analysis described here allows more flexibility than the traditional methods of discriminant analysis.

Fig. 3.7 and Fig. 3.8 compare the predicted and true electrofacies groups for the dolomite and sandstone formations respectively for wells with core data. The distinct clusters defined based on the unique characteristic of the well logs measurements are electrofacies obtained from the model-based clustering method. The predicted electrofacies groups are from the discriminant analysis using the

proposed methodology. The prediction results shown an exact match with the electrofacies groups obtained from the clustering.

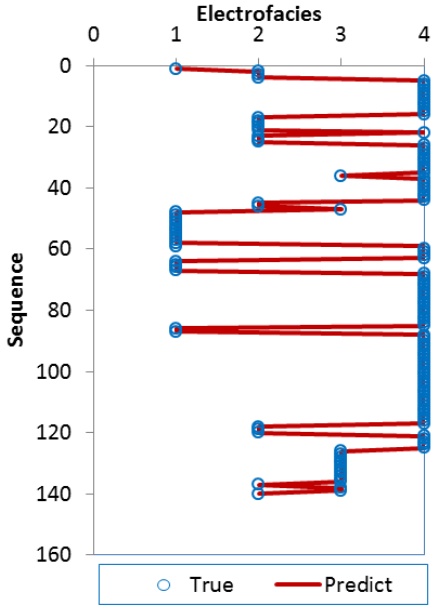

Fig. 3.7 - Predicted vs. true electrofacies. (Dolomite)

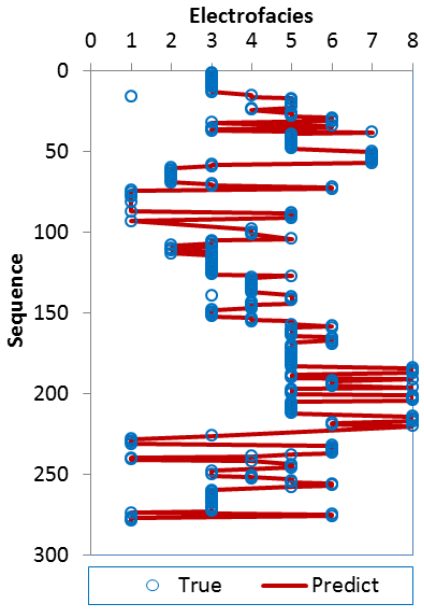

Fig. 3.8 - Predicted vs. true electrofacies. (Sandstone)

3.8 Transform Models

We use regression models to explore the causal relationships between the permeability and porosity from the well logs. The regression models will provide the conditional expectations of the well log responses given that the independent variables varied. The general form of the regression model is represented by *n* number of independent variables (X_1, … X_n), with the regression coefficients, $a_o, a_1, \ldots, a_n$ and a response Y given as follows.

$$Y = a_o + \sum_i^n a_i X_i + \varepsilon \tag{18}$$

where ε is the error term. In this case, the regression model assumes that the dependent variable is varied with combinatory linear functions of the well log measurements. This multiple parametric regression

approach can be validated provided that the assumed functions between the well logs and the dependent variables are appropriate. We used the non-parametric regression techniques to overcome the shortcoming of the regression models to predict the porosity and permeability from the wells.

Alternating Conditioning Expectation (ACE) algorithm is a non-parametric regression techniques that was developed by Breiman and Friedman (1985). The ACE algorithm maximizes the correlation between the dependent and independent variables by estimating the optimal transformation for multiple regressions of the variables. This ACE regression model was first proposed for data correlation to estimate permeability statistically from the well logs without knowledge of the functional relationship between the petrophysical properties of the rock. (Lee and Datta-Gupta, 1999;Lee et al., 2002;Mathisen et al., 2003b;Taware et al., 2008). For a given dataset, an ACE regression model has the general form with $\theta(Y)$ as the function of the response variable, and ϕ_i (X_i) are the functions of the well logs predictors as seen in Eqn. 19.

$$\theta(Y) = \alpha + \sum_{i=1}^{n} \phi_i(X_i) + \varepsilon \tag{19}$$

ACE model replaces the problem of estimating the linear combination functions of variable X by estimating the separate functions $\theta(Y)$ and ϕ_i (X_i) using an iterative method. In this algorithm, the transformation functions $\theta(Y)$ and ϕ_i **(**X_i) are achieved by minimizing the unexplained variance of the relationship between the transformed respond variables and the transformed predictor variables. The unexplained error variance $\left(\varepsilon^2\right)$ by the regression of the transformed dependent variable on the sum of transformed independent variables is given as follows.

$$\varepsilon^2\left(\theta, \phi_i, \ldots, \phi_p\right) = E\left[\theta(Y) - \sum_{i=1}^{n} \phi_i X_i\right]^2 \tag{20}$$

The minimization of ε^2 with respect to the functions $\theta(Y)$ and ϕ_i (X_i) is carried out through a series of single function minimizations involving in two mathematical operations of conditional expectations and iterative minimization as shown as follows.

$$\phi_i(X_i) = E\left[\theta(Y) - \sum_{j\neq 1}^{N} \phi_j X_j \middle| X_i\right]^2$$

$$\theta(Y) = \frac{E\left[\sum_{i=1}^{N} \phi_i X_i | Y\right]}{\left\| E\left[\sum_{i=1}^{N} \phi_i X_i | Y\right] \right\|} \tag{21}$$

After the minimization process, the estimated optimal transformation of $\phi_i^*(X_i)$ and $\theta^*(Y)$ in the transform space is related as shown in Eqn. 22. The error term, e^*, is the error not captured by the ACE transformation and is assumed to have a normal distribution with zero mean.

$$\theta^*(Y) = \sum_{i=1}^{n} \phi_i^*(X_i) + e^* \tag{22}$$

ACE derives the optimal transformation from the dataset without prior assumption of the relationship between the predictors and the responses. Within each electrofacies, the predictors are regressed with well log measurements and the derived transforms are used to predict the porosity and permeability from the well logs. We developed the transforms models using the proposed method to obtain the porosity and permeability and the results have been validated with core measurement.

3.9 Validation and Field Applications: Ogallah Field

We validated the model based discriminant analysis model by re-predicting the electrofacies groups in the cored wells. Fig. 3.9 (1-a &b) shows the training and test dataset of dolomite and sandstone. Half of the cored wells were withheld from the training dataset, and used to predict the electrofacies group of the other half. Fig. 3.9 (2-a & b) shows the predicted electrofacies groups. The prediction results show high accuracy with one data point being misclassified.

We present the field application results using the proposed methodologies for the Ogallah field data. This field contains two reservoir units with two different depositional characteristics. These heterogeneous reservoirs are Arbuckle carbonate and sandstone formations. The field consists of 111 wells, out of which 18 wells had core analysis data. The carbonate reservoir is mainly dolomite, with four identified lithofacies namely, argillaceous dolomite, crystalline dolomite, limy dolomite and sandy dolomite. In the sandstone reservoir, seven lithofacies of sand, argillaceous sand, calcite sand, dolomitic sand, limy sand, medium sand and coarse sand were identified from the core analysis data. The petrophysical classification of the core focuses on visible descriptions of the core samples which cannot be defined in depositional or digenetic terms. We considered the field wide availability of the well logs

and selected a well log suite which consisted of: gamma ray (GR), lateral log (R_t) and microresistivity log (R_{xo}) for electrofacies characterization.

The porosities are predicted using well logs by the methodology described for cored data and are compared to the cored porosities, as shown in Fig. 3.10 and Fig. 3.11. The predicted porosities showed a goodness of fit of 37% and 43%, for dolomite and sandstone respectively. These values showed a marked improvement as compared to porosities predicted using average m values ($R^2 < 0$) for dolomite and sandstone.

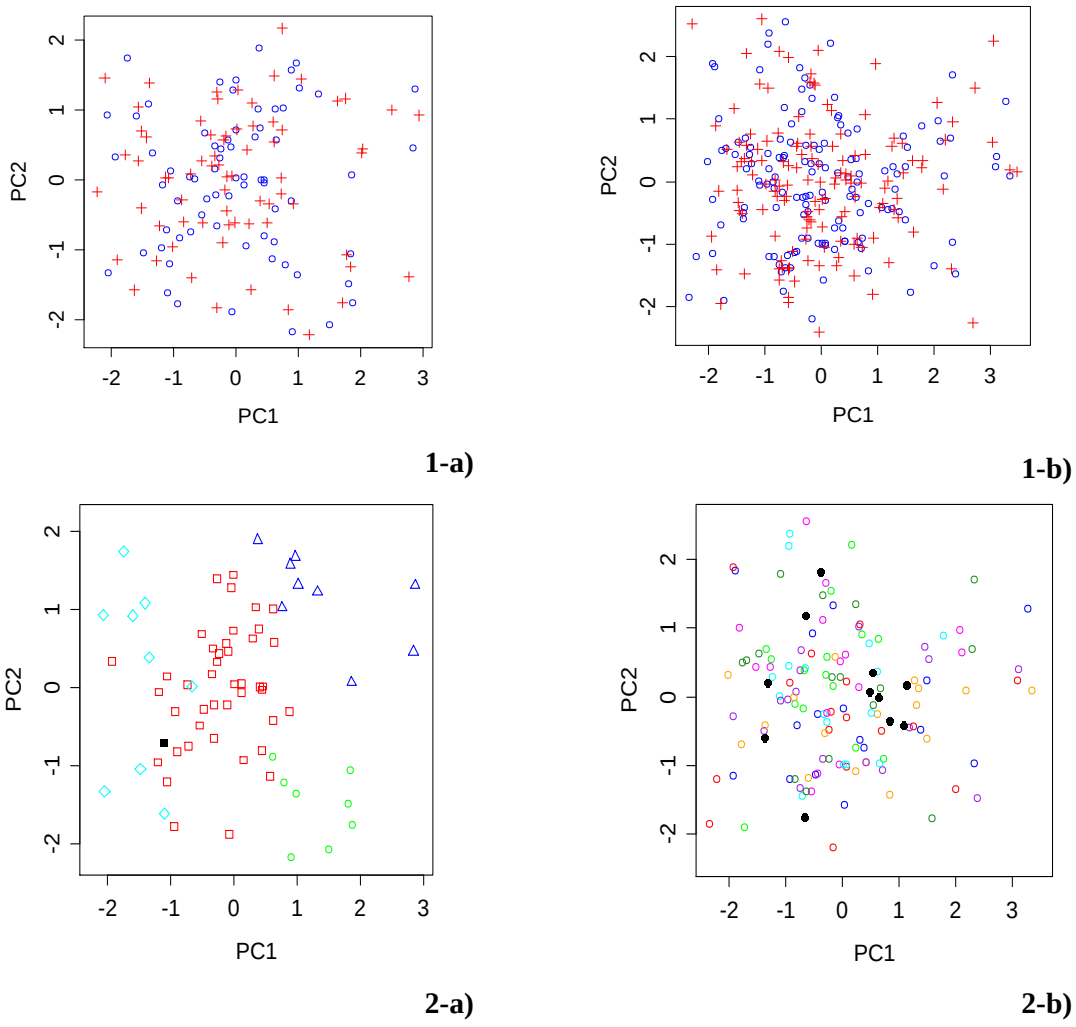

Fig. 3.9 - Test and train data. Cross is train data and circle is test data. 1-a) dolomite; 1-b) sandstone. Test error shown as filled circle. 2-a) dolomite ~ 0; 2-b) sandstone ~ 5.4%.

It is noteworthy that the permeability distribution in each electrofacies showed a normal distribution only after a log transformation. The results of the permeability prediction are shown in Fig. 3.12 and Fig. 3.13 for dolomite and sandstone, respectively. The sample number is indicated as indices. The prediction has a goodness of fit R^2 of 0.32 for dolomite and 0.62 for sandstone. The R^2 values using a simple semi-log porosity-permeability relationship were 0 for dolomite and 0.53 for sandstone. The methodology proposed here shows a marked improvement over the permeability predictions using simple semi-log porosity-permeability relationships for carbonate, as seen in Fig. 3.14**.** The permeability predictions are especially good for crystalline dolomite and sandy and argillaceous dolomite, likely due to the absence of interfering factors like unconnected vugs. For sandstone, the predictions using a simple semi-log relationship are comparable to those obtained from the approach described; this is understandable given the relative homogeneity in the porosity-permeability data of sandstone.

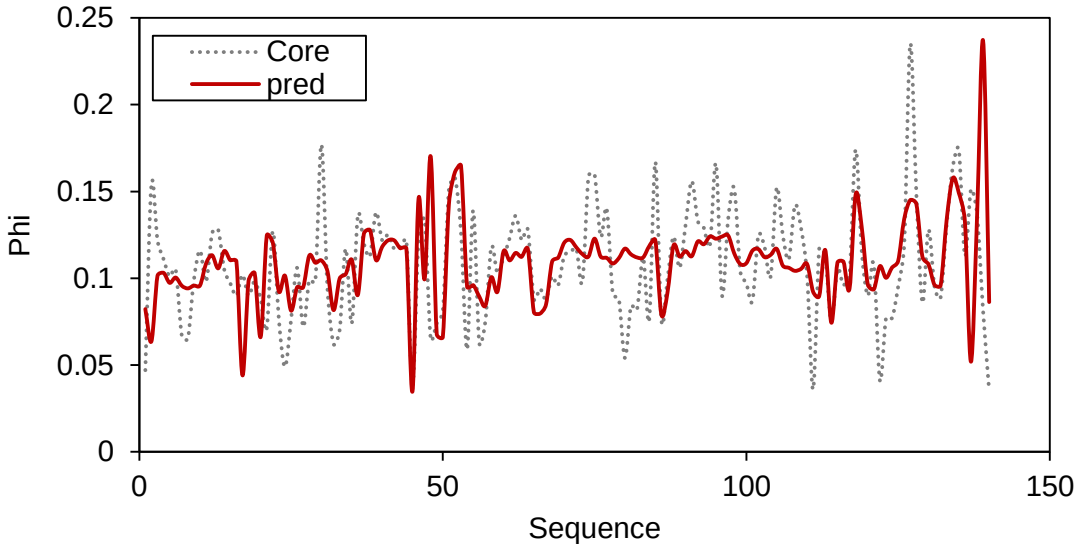

Fig. 3.10 - Measured vs. predicted porosity based on m values and electrofacies classification. (dolomite)

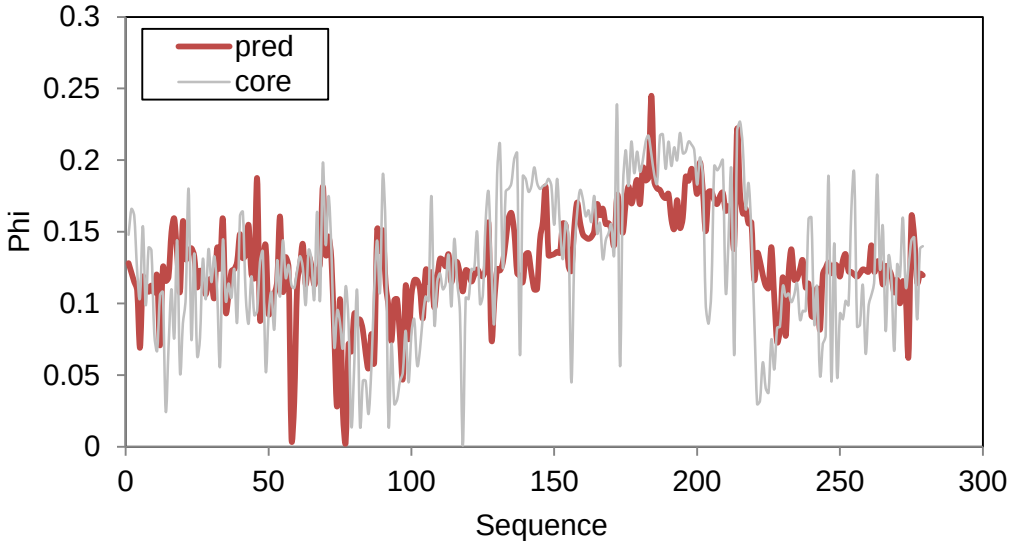

Fig. 3.11 - Predicted vs. measured porosity based on m values and electrofacies classification. (sandstone)

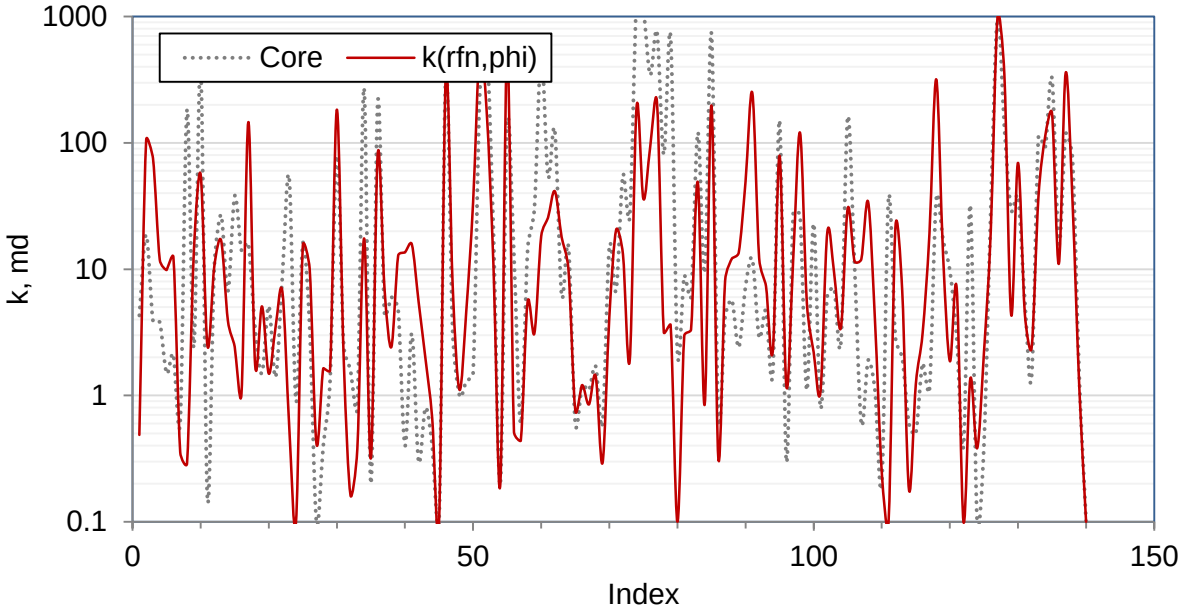

Fig. 3.12 - Measured vs. predicted permeability based on *rfn* classification and electrofacies. (Dolomite)

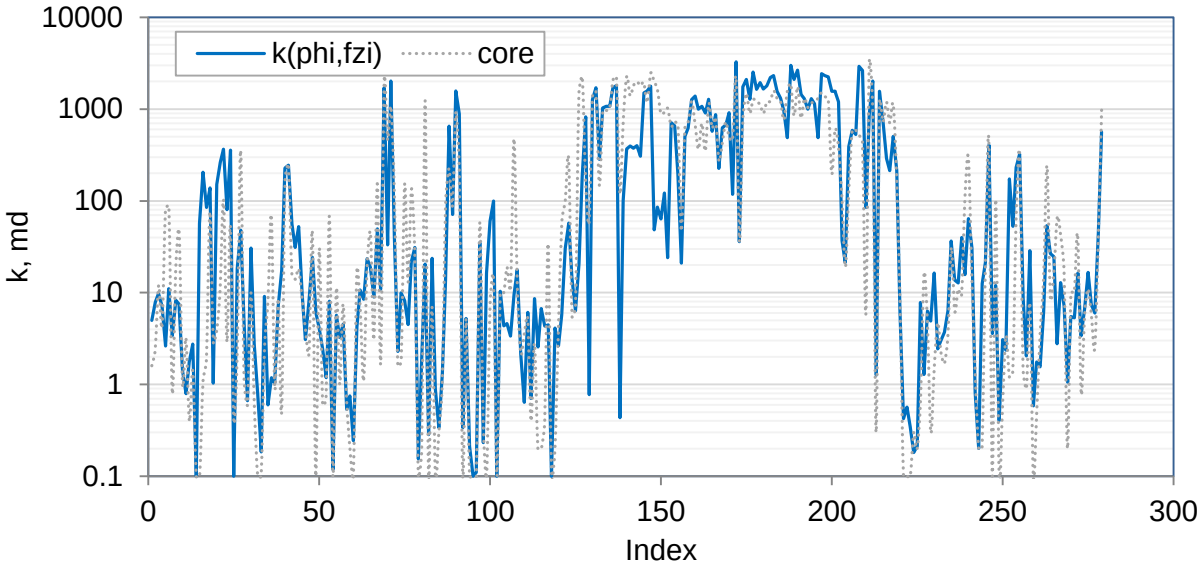

Fig. 3.13 - Measured vs. predicted permeability based on fzi classification and electrofacies. (Sandstone)

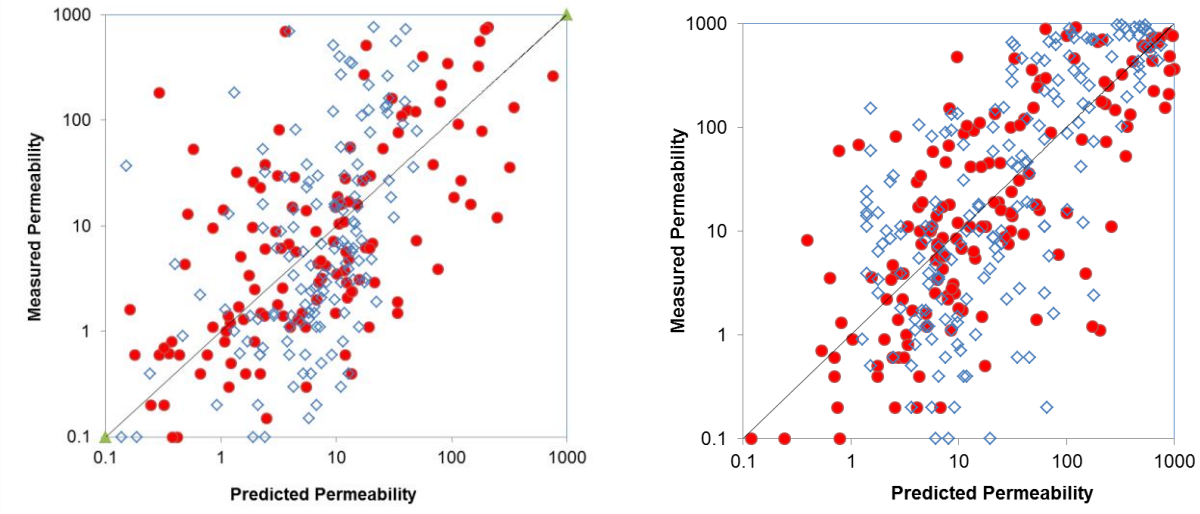

(a) **(b)**

Fig. 3.14 – Comparison of measured and predicted permeability (a) dolomite; (b) sandstone.

3.10 Summary

A data-driven methodology was developed to characterize a reservoir with limited data, and applied to the Ogallah field. In this section, the core data are integrated with well logs using the proposed methodology and the heterogeneity of the pore characteristic was identified and quantified using the petrophysical classfiers, which quantify porosity-permeability relationship. The petrophysical classifiers of the carbonate and sandstone were identified as rock fabric numbers and FZI respectively. Value of m and petrophysical classifiers have a linear correlation; both represent pore connectivity. These parameters are correlated with well logs and extended across the field. The well log data were classified into electrofacies, using multivariate analysis and these electrofacies were found to have a close correspondence with the lithofacies identified from core data. The correlations between m/classifier and well logs were developed within each lithofacies. Permeability and porosity were predicted at the well locations and results showed improvement over simple linear fit for both k and phi prediction. An understanding and incorporation of this methodology is expected to improve results in reservoir characterization.

CHAPTER 4

RESERVOIR MODELING AND HISTORY MATCHING

4.1 Summary

The process of reservoir characterization begins with defining the reservoir petrophysical properties through incorporation and integration of well logs, core data and other sources of geological information. The gathered information is then used to populate an initial model for simulation, leading to better reservoir management. In this chapter, we simulate the production performance using the model and validate the model with history matching. History matching is a process of incorporating dynamic data into a reservoir model. The process of history matching is generally a trial and error method where the properties provided by an initial model are modified until a match is obtained between the reservoir simulation results and the field production data.

In Chapter 2 and 3, we described an integrated methodology combining cluster analysis, geostatistical methods and practical aspects of reservoir engineering to incorporate static data. We applied model based clustering methods to the well logs and utilized the transform relationship between core and well logs to predict porosity, permeability and rock type in the reservoir. The approach was applied to the Ogallah field, a Cambrian formation, which is a carbonate-sandstone reservoir with 60 years of production history. Section 4.3 discusses the well logs and core properties that are concerned with the model construction. Section 4.4 discusses geostatistical methods applied to extend the petrophysical properties and characteristics of the reservoir to inter-well areas using the porosity and permeability profile predicted for 119 wells in the study area.

We utilized the reservoir characterization results to construct a black oil reservoir simulation model to history match the field performance of 60 years production period, which is described in Sections 4.5 and 4.6. We discussed the improvement of the integrated reservoir model using the proposed methodology as compared to simplified reservoir models in Section 4.7. During the history matching process, the simulated results were matched with the production history without modification of the geological heterogeneity identified through the reservoir characterization. A good history match of field, lease and individual well productions were obtained for most of the area as shown in section 4.8 and 4.9. Through the simulation results, we validated the integrated reservoir characterization approach in the field application of the Ogallah field.

4.2 Introduction

The approach used for history matching is as follows: to adjust the reservoir parameters according to their degree of sensitivity and uncertainty and thereby leave out the ineffective parameters, in order to lead to an improved solution with minimum changes to the parameters, using automated history matching methods if necessary. The problem involves essential understanding of a) practical purposes and acceptability requirements of the reservoir model b) quality of the reservoir model and the production data c) design or redesign of well-justified objective functions or history matched parameters d) adequate parameterization considering the main uncertainties and their effect on the simulation results e) proper sampling of the representations of the reservoir properties f) screening the uncertainty space; and g) judicious evaluation of results from the previous steps of the history-matching process. The objective function was minimized using algorithms, which may be broadly classified into 4 different types: gradient-based methods, global objective stochastic methods and data assimilation approaches such as ensemble Kalman-filter.

Application of ensemble Kalman-filter is typically used to include geophysical models for history matching to assist data assimilation in large scale systems (Aanonsen et al., 2009;Seiler et al., 2009;Emerick and Reynolds, 2011). Gradient-based-methods searches optimal parameters using the gradient of the objective functions; Stochastic data-integration methods are nonintrusive iterative workflows, which use a stochastic sampling optimizer to history match the seismic data and production to produce more predictive reservoir models (Alpak and Kats, 2009;Schulze-Riegert et al., 2009). The reservoir dynamics were described using methods like finite-difference or streamline simulation. Streamline simulation is a method to carry out the fluid flow simulation in a reservoir where the fluid is transported along the streamlines, which are obtained at each time step. Streamlines identify drainage and irrigation volumes, which guide the modification of static-grid-block petrophysical properties in history matching (Thiele et al., 2010). Most of the published contributions include synthetic examples or field cases to demonstrate successful application of the algorithms and simulation methods.

In this study, we developed an integrated methodology where the history matching is performed while honoring the heterogeneity and continuity in petrophysical properties obtained from static data, rather than relying on the computational power of automated methods to achieve an accurate production match. Thus, we specifically address the reservoir design issue as it pertains to the simulation of the recovery processes. Based on the systematic methodologies that we used to define the petrophysical properties of the reservoir model, we demonstrated that an improved reservoir description provides a simplified route to obtain a history-matched model which is also predictive. The developed methodology

was applied in a reservoir simulation model to history match the production performance of a 23 mi^2 area containing 114 wells in the Ogallah reservoir. Production is primarily from the carbonate and sandstone reservoir. The model was constructed using 101,100 gridblocks and used to match 60 years of production history from 1951 to 2009. From 1951 to 1969, the Ogallah field was under proration orders regulated by the Kansas Corporate Commission. The proration rate for these period of time was about 25-40 bbl/day, and production from each lease was restricted to the sum of the prorated rates for individual wells. The proration constraint was removed when the field was unitized in 1969, and the wells were operated under bottom hole pressure constraints from 1969 to present with a producing WOR of 100 as economic limit of waterflood.

4.3 Well Logs and Core Data

There are 111 well logs from the wells in the field. The producing formation is a dual-reservoir unit system with carbonate-dolomite of Upper Cambrian age, which overlies and grades downward into sandstone (Reagan). Through gamma ray log, the contact of sandstone with the underlying Precambrian rock is found to be sharp and distinct, whereas the contact with the overlying Arbuckle Group was gradational and discernible. This sandstone overlies unconformable Precambrian crystalline rocks (Granite Wash). The wells are logged at 10 – 25 ft into the formation and many of the wells do not have a complete well log suite. The complete well logs suite selected for reservoir characterization were gamma ray, resistivity and microresistivity logs after consideration of the physical measurements of the well logs and log availability in each well. Wells which fulfilled these selection criteria were located in the surrounding region but absent in the center of the field. We applied multivariate statistical analysis to the selected well logs and integrated them with the petrophysical properties from core data to predict the petrophysical property profiles at wells.

Core data were found for 18 wells that cored between 3948 to 4080 ft. Three wells were located at the center of the study area with partial penetration into the producing formation. Porosity and permeability measurements were taken from cores (average 35 ft) at 0.5 ft sampling intervals. From the core analysis description, it is clear that the basal sandstone grades upward into a dolomitic sandstone and to a sandy dolomite and, above the described interval, into dolomite. The highest thickness of the sandstone is about 34 feet in well 11-9, which includes the interval from 3982.5 to 4012.5 feet. Dolomite occurs throughout the cored interval and is about 10 to 34 ft. The dolomitic content increased in the upper few feet of the sandstone to about fifty percent of the rock. The formation contains silica in the

form of intergranular cement and quartz overgrowths. Calcite is present in local areas both as an intergranular cement and as filling with presence of vugs. Siderite and limonite are present together locally. In addition, limonite is also present in fractures.

Quartzose sandstone forms a majority of the basal sandstone, with feldspathic sandstone and arkose present in the remaining part. The sandstone color varies from red, gray, pink, buff or white depending on the amount of feldspar and nature and amount of cementing material. Grain size of the sandstone ranges from fine to very coarse, with scattered granules and pebbles of quartz and feldspar. The larger quartz grains are rounded and frosted and contain inclusions of magnetite, garnet, and potassium feldspar. Many of the smaller grains are angular to subangular and have clear surfaces resulting from secondary quartz overgrowths. The sorting of the basal sandstone varies from good to poor. The least degree of sorting is found in the coarse layers. Thickness of bedding ranges from laminae to thin beds, where the laminae consist of irregular to contorted illite. The coarse layers of graded bedding generally contain grains of quartz and microcline 2 to 5 mm in diameter.

Variations in the nature, amount, and kind of cementation produce apparent "bedding" in some parts of the core. There is no uniformity with respect to the type and amount of cement in the sandstone. In general, the core displayed porosity ranges from 11 to 20 percent; permeability ranges from 0.01 to 3500 millidarcys. Variations in porosity are primarily a result of the type and amount of cementing material and, to a lesser extent, of sorting and packing. The argillaceous material is not present in sufficient quantity to affect the porosity. The porosity and permeability relationship of dolomite and sandstone is shown in Fig. 4.1. The scattered in the logarithm of permeability - porosity plot of dolomite and sandstone indicates that there are influences of the pore characteristic due to changes in the depositional environment of different lithologies. We used the core measurements to develop an understanding of the pore attributes, which in turn, defined the distinct zones that provide similar flow characteristics and the corresponding petrophysical properties as covered in earlier chapters.

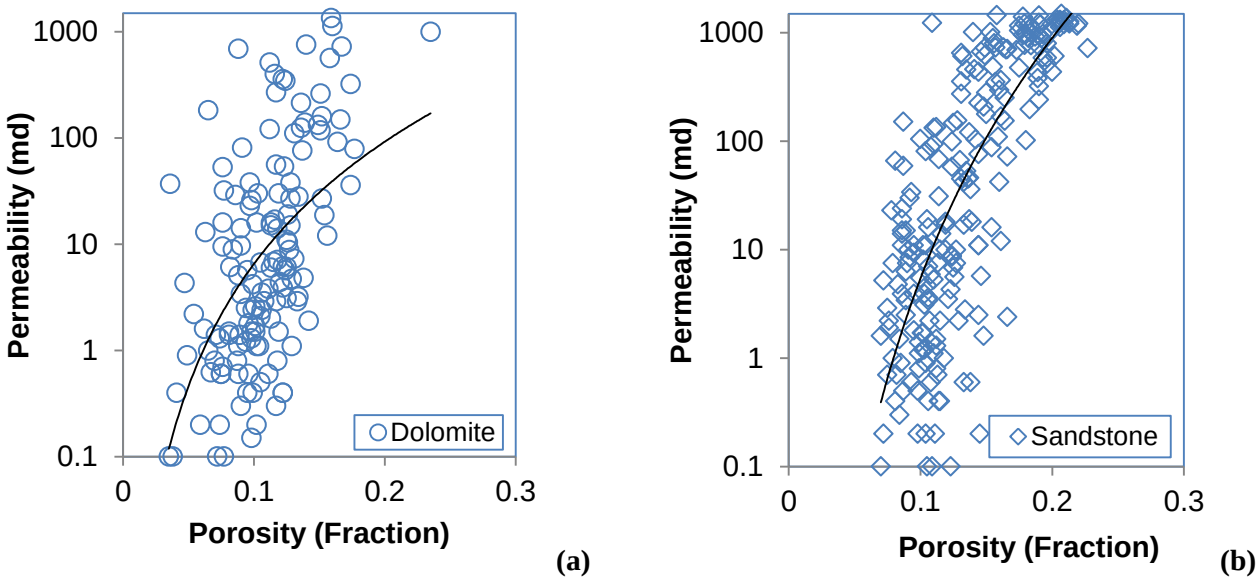

Fig. 4.1 - Core Porosity and permeability: (a) dolomite; (b) sandstone

4.4 Field Application: Ogallah Field

The Ogallah field is a dual-formation reservoir system with carbonate sequence deposited on top of sandstones. A total of 18 of the 114 wells were cored. The simulation model has 114 production wells with 60 years of production history. The reservoir area covers 14720 acres with an average thickness of the sandstone and dolomite about 20 and 25 feet respectively. Primary production of the Ogallah was initiated in 1951. No water was produced pre-1960, and breakthrough of water occurred post-1960. As water production increased, workovers were done which involved well deepening, plugging high water producing intervals and perforating upper intervals in the wellbore. At the peak of production in 1969, the Ogallah field had 85 producing wells and produced 1.07 MMBO with cumulative production of 11.37 MMBO. In 1989, half of the wells were shut-in due to economic decline. The reservoir pressure remained at about 1200 psi as a response to the aquifer support.

The Ogallah reservoir consists of 2 production units, an upper layer of dolomite formation and sandstone layer at the bottom with no shale barrier between them. The productive interval is composed mainly of dolomite for the wells located at the East and West side of the field and towards the center of the field, the sandstone interval thickens and the dolomite interval decreases. We used well logs, geological reports and core description to identify the formation markers along the wells. Porosity and permeability measurements from core are available for 13 wells. The range of the porosity is between 0.1

and 0.15 and the permeability varies considerably from 0.54 to 3750 md. There are four (4) lithofacies represents the dolomite intervals and eight (8) lithofacies represents the sandstone intervals of the reservoir. The highest quality facies is the sandstone facies with average permeability of 1881 md and the dolomite facies with average permeability of 811 md. Impermeable shale streaks were found at different locations in some wells from 3972 ft to 4078 ft which acted as a barrier for water influx from the aquifer. Some wells were produced only oil for about 10 – 15 years. Thereafter, water production increased significantly. The water oil contact is located around 1700 ft below the sea level and the total thickness of the reservoir is close to 50 ft.

Fig. 4.2 is a cross section of the Ogallah reservoir model showing wells intersecting at the dolomite intervals and sandstone intervals or both intervals. The wells at the north and south side of the field are mostly dry. There was one salt water disposal well (well 1-3) when the field was developed. Other SWD wells (Wells 6-4, 11-9, 11-10 and E-3) were converted from active producing wells to injection wells when the water oil ratio of the wells exceeded the economic limit. Most of the SWD wells were completed approximately 250 ft below the producing formation and disposal of produced water was assumed not to affect the reservoir pressure.

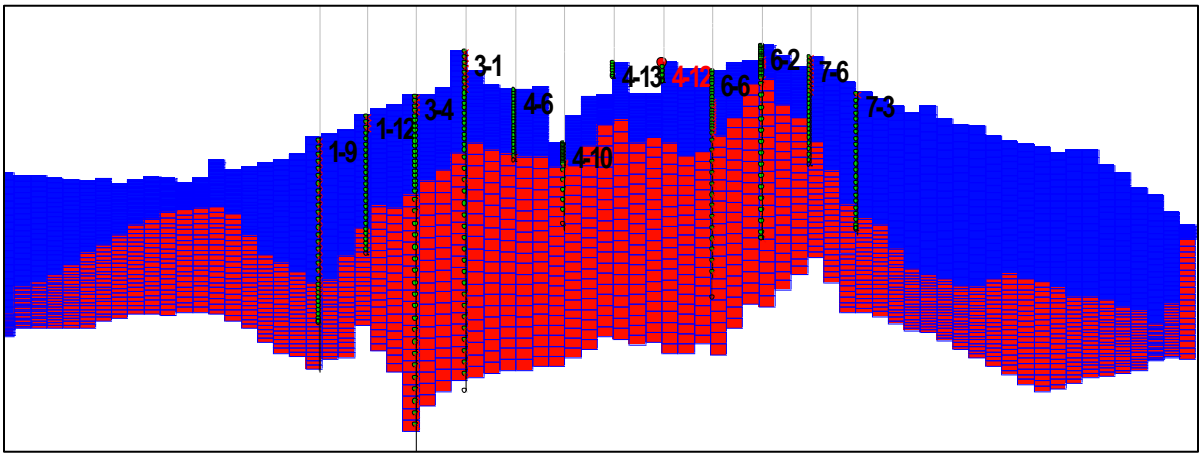

Fig. 4.2 - Cross section of wells intercepting the dolomite and sandstone intervals.

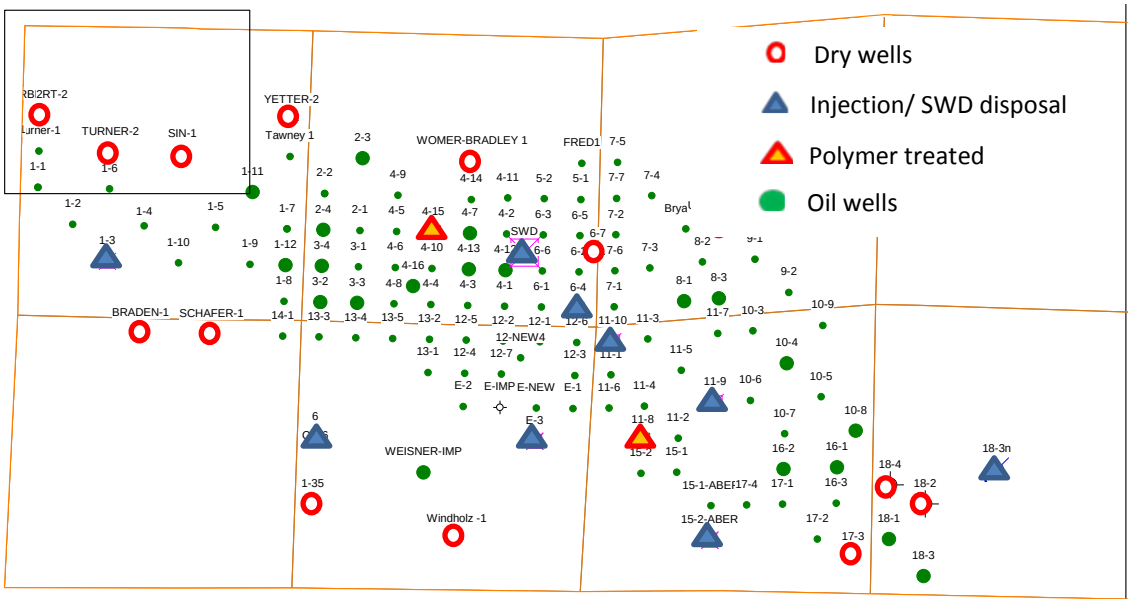

Fig. 4.3 - Ogallah field well activities and status at year 1969 to 2009.

4.5 Geostatistical Approach and Results

We utilized the porosity and permeability profile of the wells to characterize the reservoir model with an appropriate porosity and permeability distribution. We applied a hybrid simulation approach which involves two or more conditional simulation techniques to generate more realistic reservoir descriptions. Two most popular conditional simulation techniques to describe lithofacies are object modeling and Sequential Indicator Simulation (SIS). Object modeling is recommended for fluvial, deltaic and deep marine depositional environments and the shape of main lithofacies in these environments (like channels, mouth bars, levees and different types of shale) can be represented by discrete objects with unique shapes. Use of object modeling requires information describing various geological objects without which the method cannot produce realistic results. In this study, a hybrid simulation approach is applied to describe the dominant lithofacies and correlations of the petrophysical properties in their depositional environment. We utilized the description of rock and shale from the core analysis and calculated the fraction volume of shale and lithofacies content for each lithotype. We attempted object modeling to quantify the distribution of laterally continuous, but thin, sedimentary bodies in a carbonate environment. The steps are executed as the following.

1. The main geologic lithofacies is associated with object modeling. This includes lithofacies that extend across a significant region of the field. The dimensions, type of objects, volume fractions, and conditioning data are specified for each lithofacies. We describe lithotypes which includes in different lithofacies with SGS instead of SIS since it can interpret categorical variables. The variograms, volume fraction and conditioning data are specified for each lithotype within each lithofacies.
2. We generated the porosity and permeability distribution of the reservoir using Sequential Gaussian Simulation (SGS). The porosity and permeability mean value were calculated using variograms and assigned based on the conditioning data specified to each lithofacies in step 1.
3. It is difficult to use object modeling application to approximate the shape of lithofacies in carbonate because the lithofacies in the carbonate environments have gone through post-depositional processes. We applied variogram analysis to the predicted porosity and permeability profile from wells, and the SGS algorithm was conditioned to the profiles to generate distributions of porosity and permeability at interwell locations.

Variogram calculation, model fitting and reservoir property population were performed. Since reservoir parameters at the same stratigraphic horizon have more depositional similarity, the variogram for porosity population was calculated within each homogeneous lithofacies viz. carbonate and sandstone separately. Though the carbonate and sandstone were divided into distinct electrofacies, the spatial modeling was not separated based on this characterization for reasons of practical consideration related to flow simulation, grid definition etc. First, the carbonate and sandstone tops were formed by interpolating the well tops using ordinary kriging. Because of negligible anisotropy in the variance of the formation tops, an omnidirectional variogram is used to calculate the kriging parameters. The reservoir thickness was interpolated similarly.

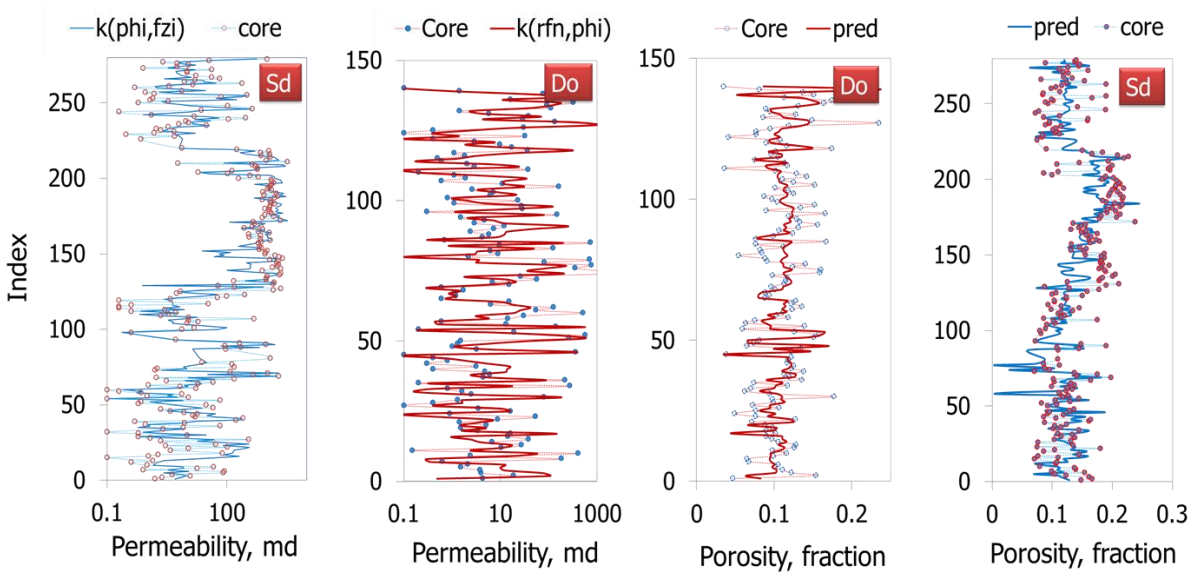

Fig. 4.4 - Porosity and permeability predicted profile.

For the porosity population in the reservoir, a bi-directional experimental variogram was calculated first. If the x and y directions were found to be similar, an omni-directional variogram was used. The experimental variograms of porosity are calculated in both vertical and horizontal directions. Since the anisotropy in the horizontal layers is negligible, an omnidirectional experimental variogram was calculated for the horizontal layers. The model variogram parameters are calculated based on the vertical distribution of the data because the sampling frequency is very low in the horizontal direction. The sampling distance in the vertical direction is 0.3 to 0.5 ft, while the shortest distance between wells in the horizontal direction is about 950 ft. A bidirectional Gaussian model variogram is used to fit the horizontal experimental variogram in two principal directions, because the spatial variance is not necessarily similar in the X and Y directions (XY is the horizontal plane). The spatial variance in the vertical direction is fit using a separate Gaussian variogram model. The nugget and sill are common to both the vertical and horizontal variograms, while their ranges are distinct. Since the data is more closely spaced in the vertical direction, the nugget and sill are calculated based on the model fit to the vertical experimental variogram. The variogram in the horizontal direction is calculated based on these values. The predominant features of the variogram observed are zonal and geometric anisotropy and cyclicity in dolomite. In sandstone, there was less anisotropy observed, though there was considerable cyclicity.

Permeability population was performed using similar Gaussian models. In the case of permeability, the models were able to simultaneously fit the experimental variograms in both horizontal and vertical directions. Once the model variograms have been fitted, it remains to populate the reservoir. Since estimation methods are accurate but smooth, simulation methods need to be used for population to accommodate several realizations which account for the uncertainty in the data. Sequential Gaussian Simulation is used to populate the porosity, and reproduce the variance in the data as shown in Fig. 4.5.

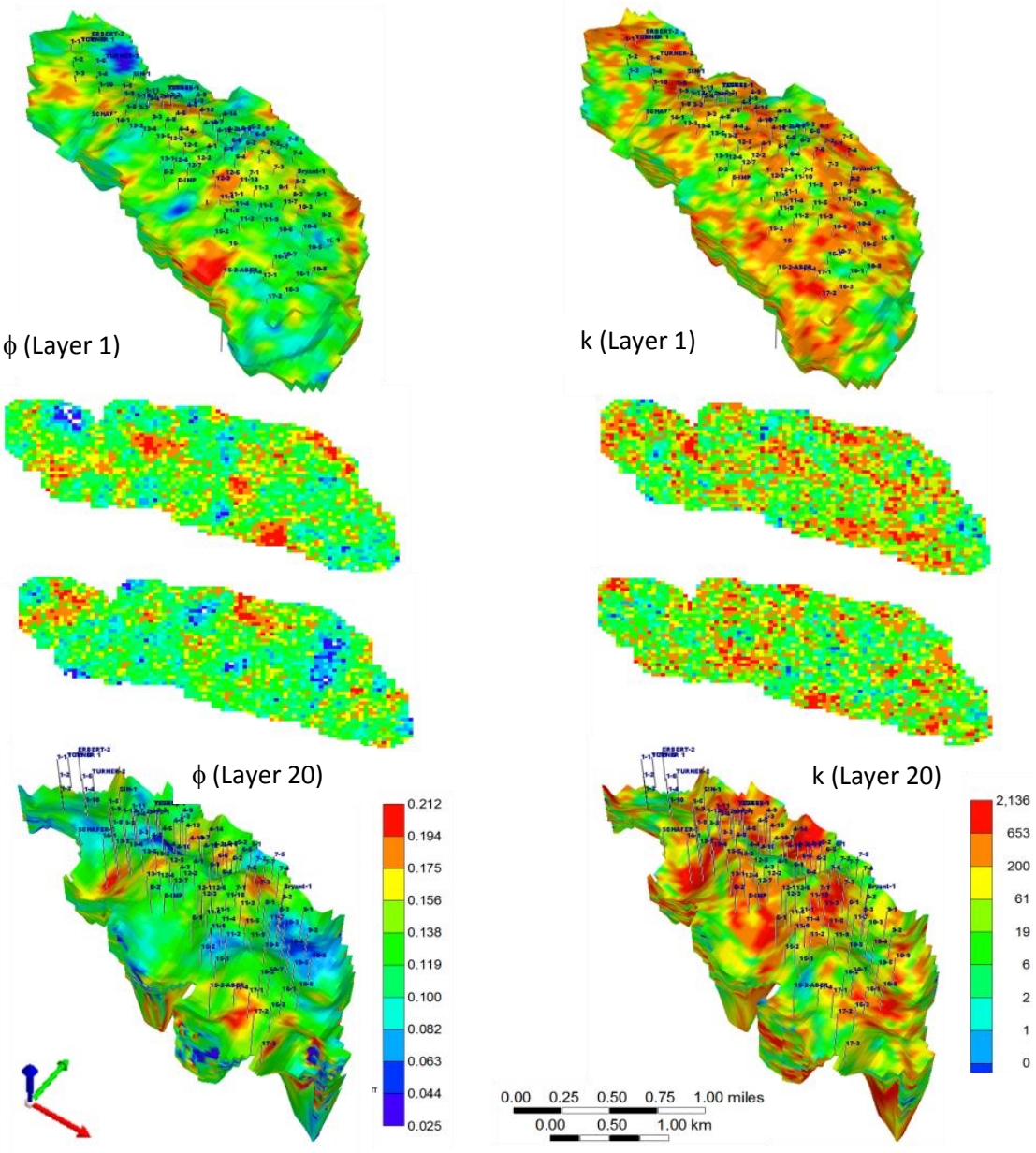

Fig. 4.5 - Porosity and permeability distribution of the Ogallah field in 3D.

Populated porosity of Layer 1 (Dolomite)

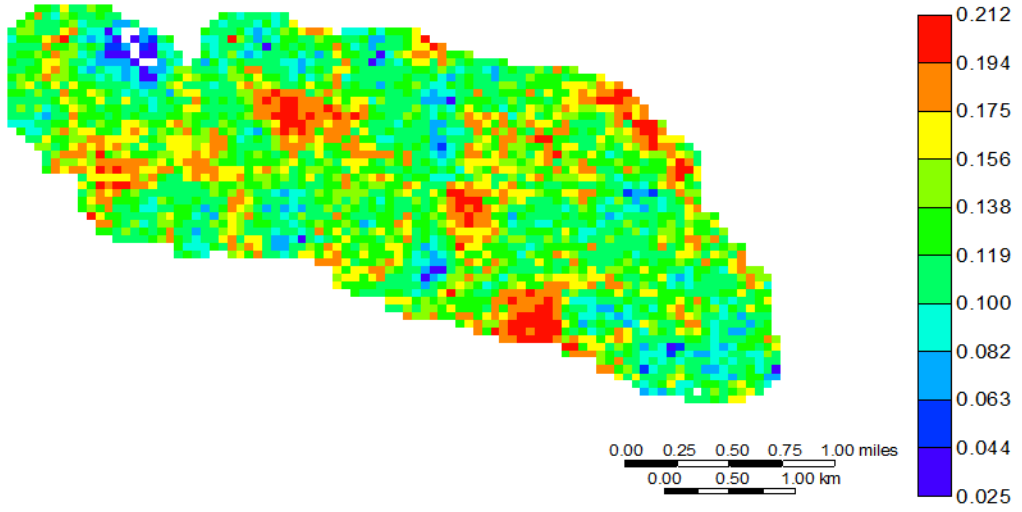

Populated porosity of Layer 21 (Sandstone)

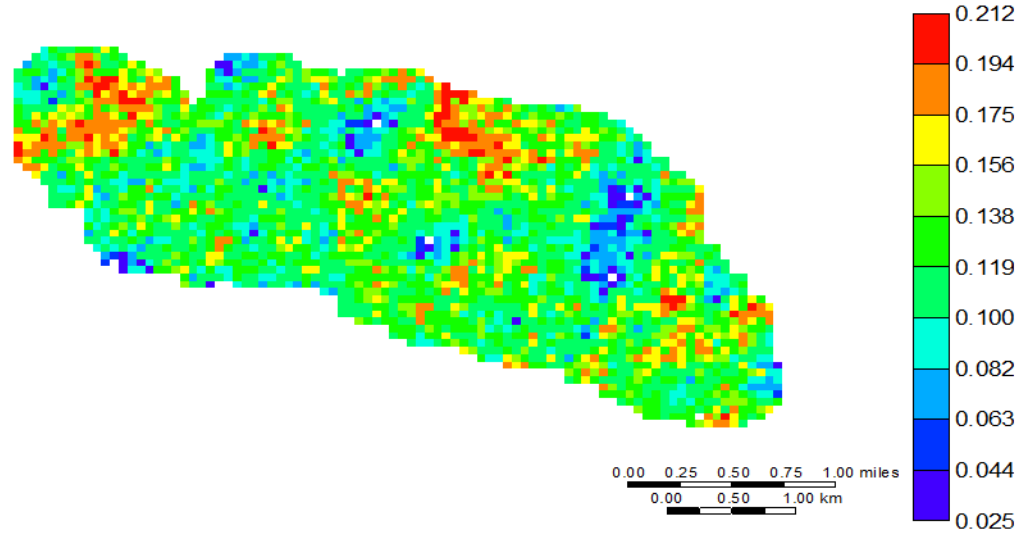

Fig. 4.6 - Porosity distribution of the Ogallah field.

Populated permeability of Layer 1 (Dolomite)

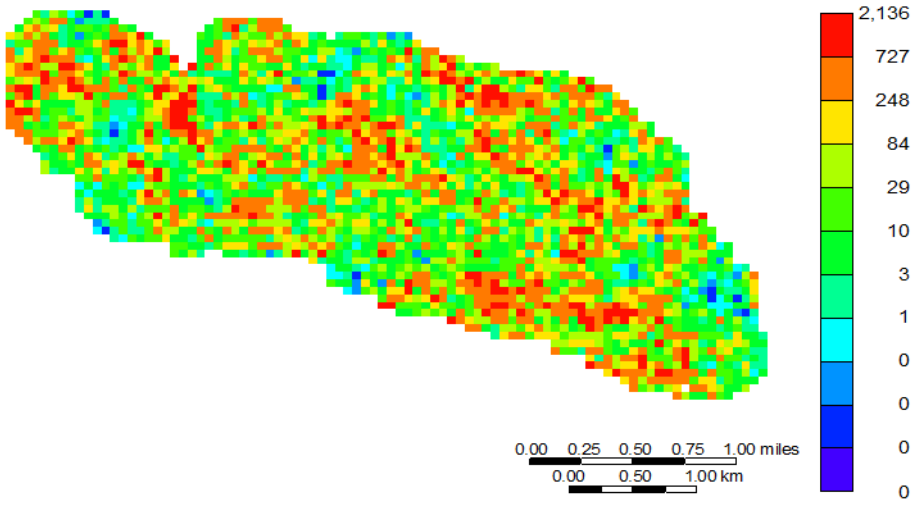

Populated permeability of Layer 21 (sandstone)

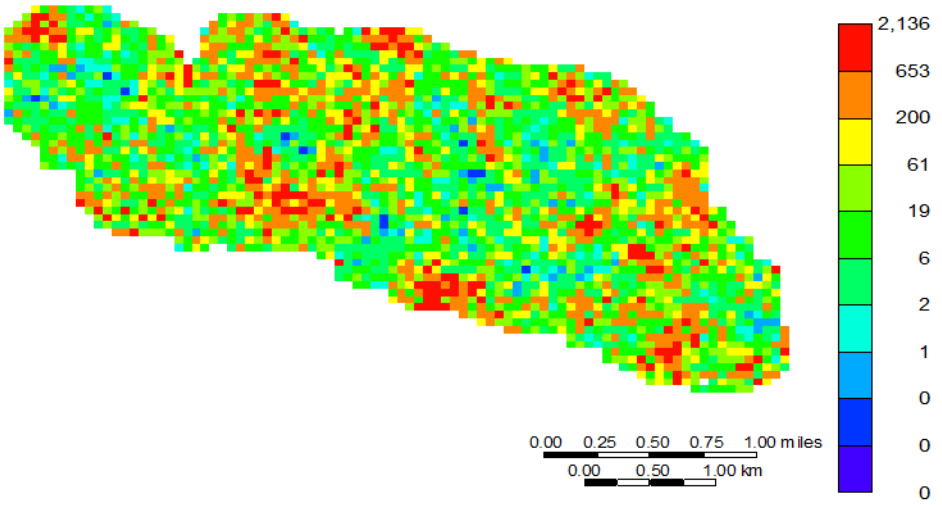

Fig. 4.7 - Permeability distribution of the Ogallah field.

4.6 Simulation and History Matching Methodology

Usually, the only way to test a reservoir model is to simulate past performance and compare the two; this procedure is called history matching. History matching involves altering the petrophysical properties of the reservoir, till the model is forced to simulate historical performance. If the alterations made in the model are consistent with the geological heterogeneities and continuity identified from well logs and cores, it can be used as a powerful tool for predictive analysis. The data needed for history matching are initial estimates of the porosity and permeability distribution in the reservoir, relative permeability, the aquifer extent, porosity and transmissibility. The data matched during the history matching process include pressure, water-oil ratio (WOR), and water arrival time. History matching of WOR is usually the best way to confirm the validity of estimates of effective zonation and zonal continuity (Mattax and Dalton, 1990). The parameters that are adjusted during history matching are aquifer transmissibility, aquifer storage, reservoir permeability including anisotropy, relative permeability, capillary-pressure functions, reservoir permeability and thickness, structural definition, rock compressibility, oil and gas properties, water oil contacts and water properties. Reservoir porosity is assumed to be reasonable and consistent to the assumed reservoir description.

4.6.1 Matching Fluid Movement for Field

In manual history matching, the permeability is the principal reservoir parameter used to obtain an adequate match of fluid movement. In automatic history matching, an objective function which defines the squared error between the simulation and history in WOR, is minimized using non-linear optimization methods. Multiple solutions to the minimization problem are obtained and all the solutions are studied in view of the uncertainty in the properties of the model. Some examples of existing algorithms used to solve the problem are gradient-based methods, stochastic methods and Kalman-Filter approaches. In this study, manual history matching is first used to understand the gross-scale properties affecting the fluid flow and a hybrid of combinatorial optimization techniques is used to refine the solution.

We verify the validity of the reservoir description and reservoir mechanics by observing critical data like pressure changes during transient periods, pressure gradients, and water arrival times. We used the field history-dependent variables such as water arrival time, individual well's WOR behavior and known reservoir conditions such as aquifer in matching the fluid contact movement. The reservoir drive mechanisms during simulations are being analyzed to determine whether the overall reservoir pressure is achieved and has influence on the arrival time of water. The areal permeability distribution of the

reservoir and the aquifer contacts were evaluated to see if the WOR behavior was matched satisfactorily. Fig. 4.8 shows the cross section of the Ogallah field and the oil-water contact, which is driven by an underlying aquifer. The effect of permeability stratification of the reservoir was ascertained to see whether vertical permeability influences the observed production history. Increased value of vertical permeability will lower the sweep efficiency and thus delay the water arrival time.

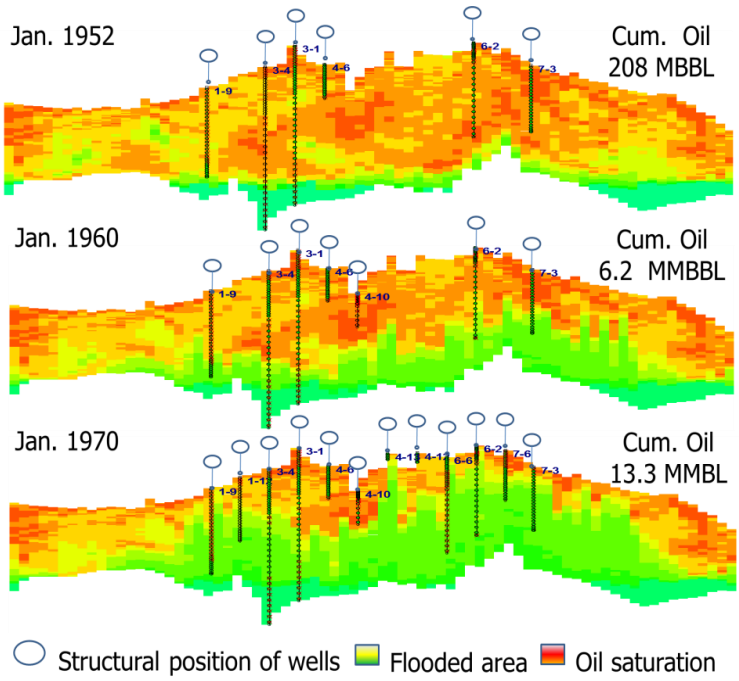

Fig. 4.8 - Water-oil-contact movement (depletion behavior) of the Ogallah Reservoir.

4.6.2 Sensitivity of Parameters for Individual Well

In this section, we illustrate the problems from the production history mismatch and indicate the considerations involved to obtain a match in individual wells. Although the behavior of the reservoir simulation model could be influenced by large number of reservoir parameters, a history match is more critically affected by the actual range of effective parameters for example the permeability distribution at different regions. Recognizing the effective parameters that influence the field or individual well behavior may shorten the process of achieving precise agreement between the simulated results and production history. This step is rarely an automated process but rather based on the knowledge of the reservoir and structured approach of making such decision to achieve a production history match. The

lack of sensitivity of a parameter on the simulation could be caused by an actual feature of the reservoir which is not being included in the flow simulation or because of the uncertainty in the range of the effective parameters.

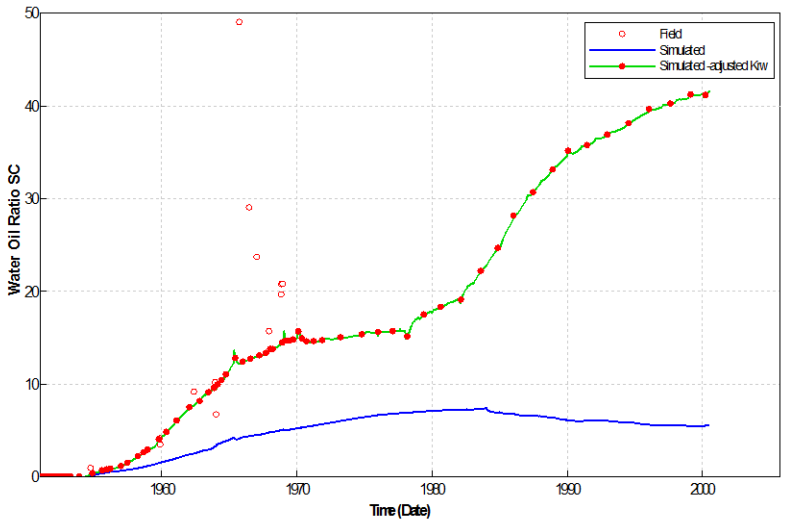

Fig. 4.9 - Well 1-6 history-match WOR. Modify water relative permeability in the well function to adjust WOR.

For instance, Fig. 4.9 shows well 1-6 in which the simulated WOR does not have the same trend with the observed data. To improve the match, adjustment of the water relative permeability curve in the well was used. The changes made on the relative permeability curves enabled the simulation from adjusted flow to converge to a satisfactory history match at the individual well level. In the initial simulation run, the horizontal permeability from the extreme rock properties has been assigned with known acceptable accuracy to eliminate necessity for alteration during the simulation. The relative permeability data poses the greatest uncertainty since there is no separate relative permeability curve available to represent each significant rock type. Therefore, adjustment of relative permeability curves is needed to match the water phase displacement. Varying absolute permeability of the reservoir is not necessary in this case. Using this procedure to understand the reservoir behavior shall improve the accuracy at the well level and reduce the effort in identifying the parameters to be modified in achieving the history match. The selected parameters appropriate for alteration should follow in approximate order of decreasing uncertainty. For this purpose, there are several tools available, for example, sensitivity study based on experiment design to determine the influence of the parameter values to the overall variation of the simulation results. The results from the sensitivity study of the simulation results, along

with the parameter uncertainty, will help to decide which parameters to perturb and range of perturbation for history matching. Although automatic tools are available, manual adjustment based on understanding of a reservoir is still almost always required. In the next sections, we illustrate the application of the methodologies developed in the previous sections to a field simulation model.

4.7 Reservoir Simulation Model

We generate a reservoir simulation model based on the petrophysical attributes that we developed earlier and we used it as the foundation for the models used in this study. The reservoir model simulation grid is a cartesian-model which has 101,100 active grid blocks. Fig. 4.10 shows the active gridblocks for Ogallah reservoir. The average grid size of each grid block is approximately 48400 ft^2. The grid block porosity and permeability are simulated using sequential Gaussian simulation and conditioned to well logs.

In the model, the gridblocks outside the field boundary were set to inactive status so that they are not contributing to flow. We defined the reservoir fluid properties, relative permeability and initialization to the reservoir model. Fig. 4.11 shows the assumed relative permeability curves for dolomite and sandstone formation of the reservoir. The initial oil water contact is approximate at 1700 ft below the sea level, the initial pressure of the reservoir is about 1200 psi, and the API gravity of the oil is about 36 API. The PVT data used in this study mostly came from the published literature and commonly used PVT correlations. The available fluid data and their sources are summarized in Table 4.2. Oil-water relative permeability curves are not available from the laboratory core test on representative core samples for this study.

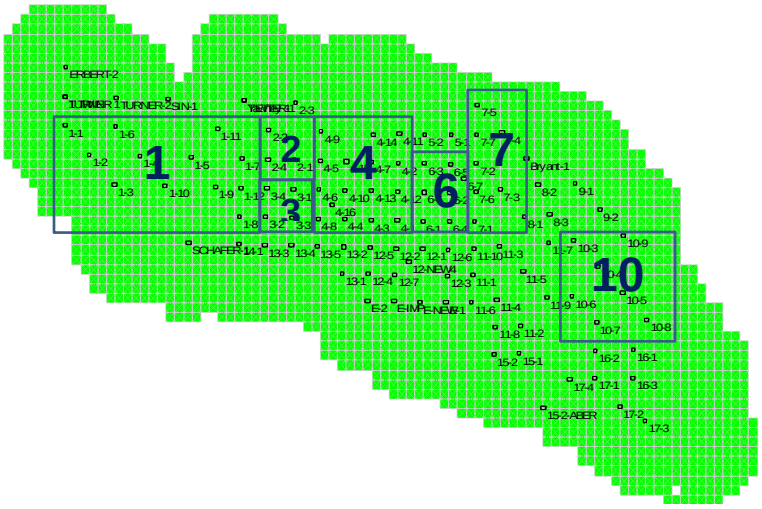

Fig. 4.10 - Grid system in the Ogallah model with the leases boundary numbered.

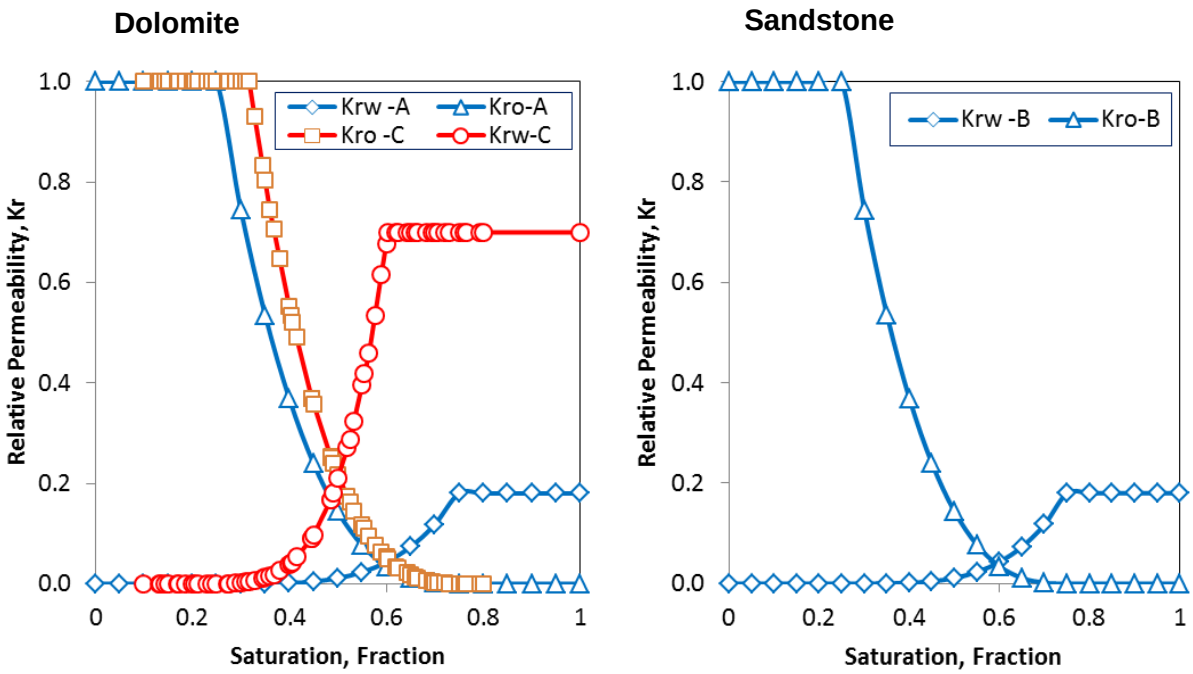

Fig. 4.11 - Relative Permeability curves used in the integrated reservoir model.

Saturation-height functions are applied to net reservoir intervals to estimate water saturation and thence hydrocarbon saturation. These functions are effective in porosity range of greater than 0.05 and

hydraulically connected reservoir zone. A saturation-height function is used in volumetric estimation of the hydrocarbon followed by the evaluation of water saturation using estimated porosity from well logs and cores. In this study, the new revelations in integrated reservoir characterization necessitate the employment of all possible reservoir data to satisfy the initialization process. The modeling of initial water saturation distribution in the simulation model is specified through a pressure and saturation at the datum depth. Table 4.2 shows the PVT parameters, which hold the initialization parameters for the reservoir. The modeling of the initial condition of the simulation model are defined by equilibration of oil and water contact and reference pressure at a datum, which determines the initial hydrostatic pressure gradients and initial saturation of oil and water phases in the model. A significant amount of study related to saturation height functions is available in the literatures (Cuddy, 1993; Skelt, 1995). These functions calculate Sw based on one or more of the parameters like porosity, oil-water contact, gas-water contact, irreducible water saturation and height above contacts. The initialization process of simulation models with representative saturation height functions renders a simulation model with consistent distribution of oil and water saturations. An accurate initialization process reduces uncertainties in the estimation of fluids in place and its distribution in the simulation reservoir, which would affect the model recovery process and in turn its reserve prediction.

4.8 History Matching Considerations and Constraints

The goal of production history matching is to understand the fluid distribution, depletion mechanism of the reservoir and to improve accuracy of the reservoir model. In Ogallah field, the data that are matched are pressure, water/oil ratio behavior, and oil production. Kansas State mandate on well tests to demonstrate the productivity of the wells during 1950s. Actual field measured data from the well test measurements (barrel test) in the field were used to describe the production performance of individual wells. From discovery in 1952 to the field is unitized in year 1968/69, production from the wells in the Ogallah field was prorated. The volume of oil per lease was restricted. A well under proration produced only for the period of time necessary to obtain the monthly allowable and then was shut in. Thus, production rates and BHP observed during the annual test are measures only of the capacity of the formation around the well and the flow characteristics of fluids entering the wellbore. Therefore the parameter adjustment in history matching is performed in two steps.

Prior to the proration, the water-oil ratio was history matched by adjusting reservoir parameters while the production was constrained to lease production. After the proration date, history matching of

the oil production data was performed by setting the bottom-hole-pressure of the producing wells. The well controls that implemented in the reservoir model following the control hierarchy is listed in Table 4.1. An aquifer was included at the bottom of the reservoir to simulate the bottom water drive mechanism and the properties of the aquifer are represented by the average of the reservoir properties.

Table 4.1 - Model controls/constraints

Field level	Well Level
Lease allowable production	Minimum BHP (28 psi)
Field production	Maximum oil production rate (30 bbl/day)

In the Ogallah field, there were no pressure data available from the production history. The flow behavior (draw-down and build-up) from drill stem test (DST) were performed at the Arbuckle formation for several wells in the drilling prognosis with two flows and two shut-ins recorded. However, the pressure data recorded in DSTs were not interpretable to determine reservoir data such as initial reservoir pressure, permeability and skin. The average pressure obtained from the initial flow period of DSTs for several wells is about 1100 psi. Regardless of difficulties in interpreting DST measurements, wells in the Ogallah field were periodically shut-in for workover and fluid level were measured which provide an estimate of average reservoir pressure. When simulating historical performance of the Ogallah field, we implemented the lease oil production rate control and allow WOR's to be calculated from the phase mobilities. Fig. 4.12 shows the production history of the Ogallah field.

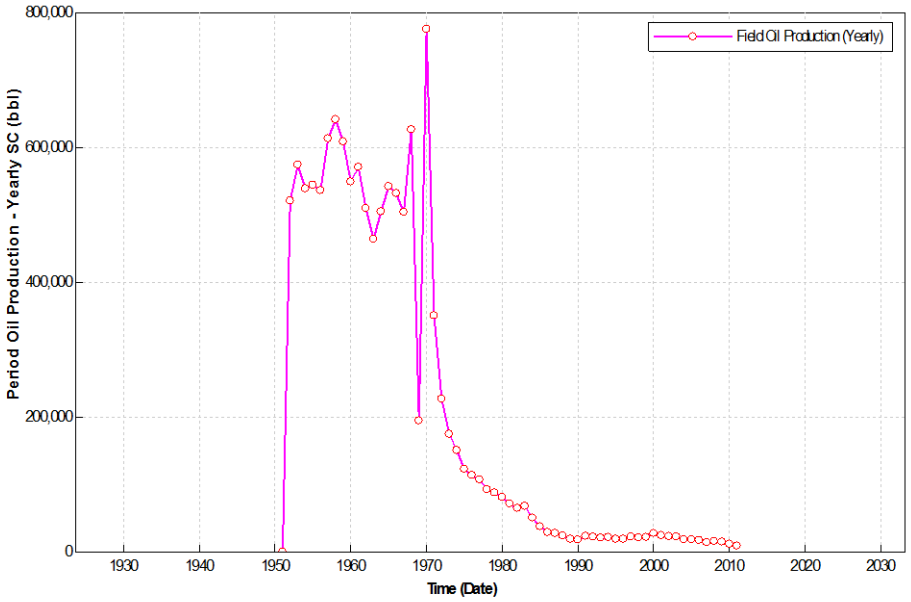

Fig. 4.12 - Ogallah field production history.

4.9 History Matching Procedure

Based on the results of the first two studies, we developed a more detailed reservoir description, where the static data was fully utilized and only those reservoir properties that were not available for the study were treated as uncertain parameters in the history matching process. This section described the properties we assess during the history matching process. The geological trend and heterogeneity features (porosity and horizontal permeability) characterized with the geostatistical approach were preserved throughout the history matching process. The details of the improved reservoir characterization have been presented in chapters 2 and 3. We characterized the petrophysical properties without conditioning the distribution to indicators which allow more variability of the petrophysical properties. Table 4.2 presents the known parameters and their corresponding value in the reservoir model. To evaluate an improved reservoir description are satisfactory to meet the objectives of the study the following parameters were chosen for alteration: a) permeability stratification; b) effects of areal permeability distribution; and c) relative permeability curves. We match the historical WOR's of the reservoir model to validate the estimates of the effective flow zone and continuity of flow zone. To predict the abandonment condition of the reservoir, we used the oil and water production from 1980 onwards to match with the simulation results.

Table 4.2 – Estimated Fixed Parameters		
Parameters	Source	Values
Reservoir temperature		110 F
Bubble point pressure calculation		14.7 psi
Oil density at STC(14.7 psia, 60 F)	Stock tank oil density	52.3967 lb/ft^3
Gas density at STC(14.7 psia, 60 F)	Gas gravity	0.67
Oil properties (Bubble point, Rs, Bo) correlations	Standing	
Oil compressibility correlation	Glaso	
Dead oil viscosity correlation	Ng and Egbogah	
Live oil viscosity correlation	Beggs and Robinson	
Gas critical properties correlation	Standing	

4.10 History Matching Results

In a reservoir simulation study, it is necessary to determine an average reservoir pressure that corresponds to the cumulative oil and water production in the Ogallah field. Fig. 4.13 shows the calculated reservoir pressure from the reservoir model with bottom water drive. The calculated pressure was consistent with the observed trend on well management. Reservoir pressure decreased rapidly when more wells were producing prior to unitization in year 1969 and recharge to 1195 psi when wells were slowly shut-in due to high water cut afterwards. The reservoir energy was primarily aquifer influx, the average pressure gradient change in the Ogallah field was low, and the pressures of the wells were about the same at any given time. There were some measured bottom hole pressure at wells over time that were reasonably close to a pseudo-steady state pressure condition of the reservoir. Fig. 4.14 shows the simulated and recorded reservoir pressure at the initial stage of producing history on a line parallel to the main direction of flow in the reservoir. Without adjustment to the reservoir model, the overall pressure of the simulation is observed to perform similar to the recorded average reservoir pressure. Bottom-hole-pressure matches for individual wells agree to within 50 -100 psi on the average.

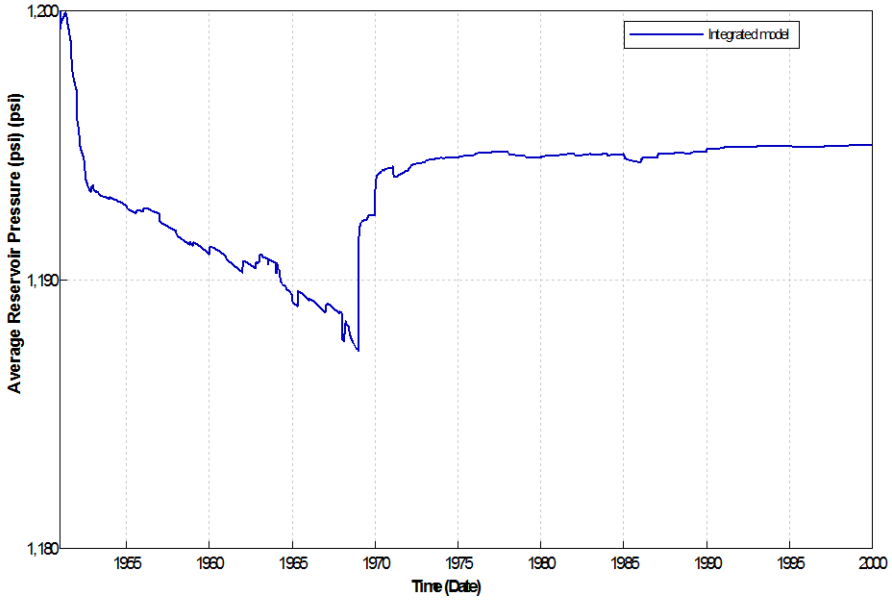

Fig. 4.13 - Average reservoir pressure of integrated model.

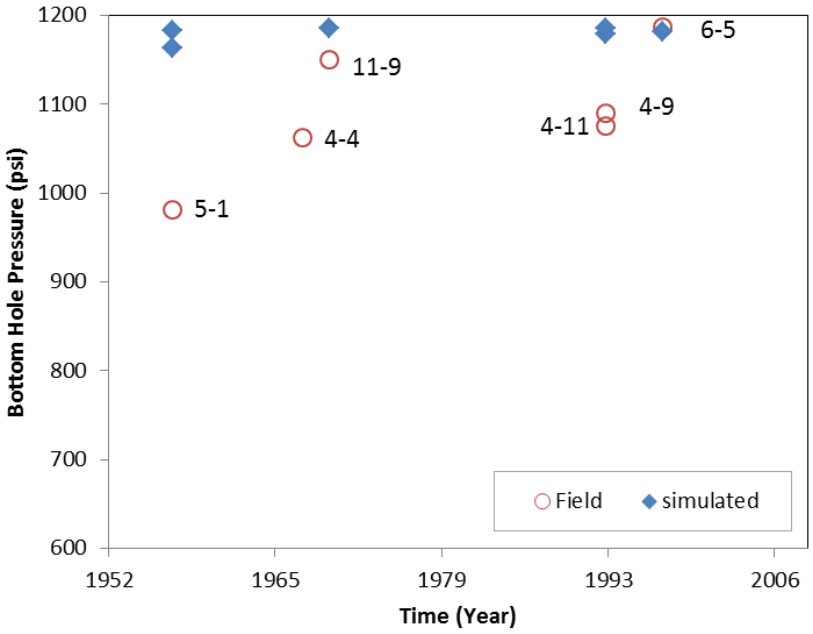

Fig. 4.14 - Measured and simulated bottom-hole pressure at well locations.

We matched the fluid movement behavior through well WOR to verify the validity of the reservoir assumptions concerning the reservoir description and producing mechanics. Fig. 4.15 shows the WOR of wells from different locations in the reservoir model. Well WORs match reasonably well for the entire field without any adjustment on the permeability and porosity. In particular, well 2-1 WOR behavior affected by shale streaks were captured. Relative permeability curves are influenced by the pore geometry, wettability, saturation history of the rock. In general the relative permeability curves which considered not reliable were modified since it has high uncertainty in matching the individual well saturation movement. From Fig. 4.15, the WOR behavior of well 6-1 and well 10-4 were history matched using relative permeability curves set C; others were matched using relatives permeability curves set A and B as seen in Fig. 4.13. The results in Fig. 4.15 were obtained by reviewing well performance individually and adjust the assumed relative permeability curves so that agreement reached between the simulated and reported fluid movement which were affected by the rock characteristics.

Fig. 4.16 illustrates the lease production history match obtained from the integrated model. We compare the history matched results with the first and second regression models on each lease. Improvement of history match at lease level was observed for all leases and overall the integrated model provides a better history match. Recovery factor during the primary recovery stage is typically 5-15%. Estimated recovery factors for all the models are shown in Table 4.3. The original oil in place calculated from the integrated model is expected to be more accurate because of rigorous prediction of porosity and saturation. The recoverable oil calculated from this model is also more accurate because of a better history match at both the field and well levels.

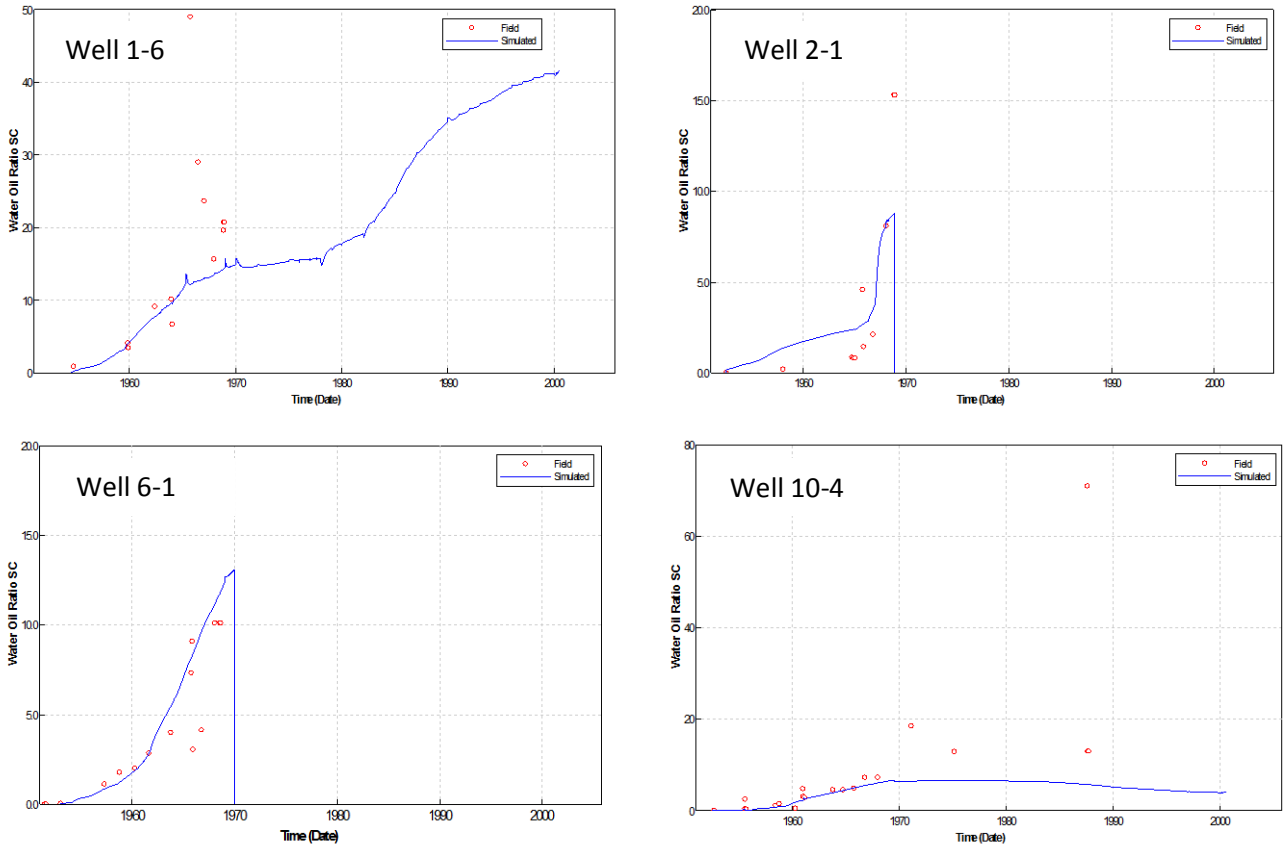

Fig. 4.15 – History-match of WOR of individual wells.

Table 4.3 – Estimated Recovery factor

	Original Oil Inplace (MSTB)	Recoverable Oil (MSTB)	RF
Simplified Model 1	23925	5747	0.24
Simplified Model 2	109917	10872	0.10
Integrated Model	77814	12835	0.16

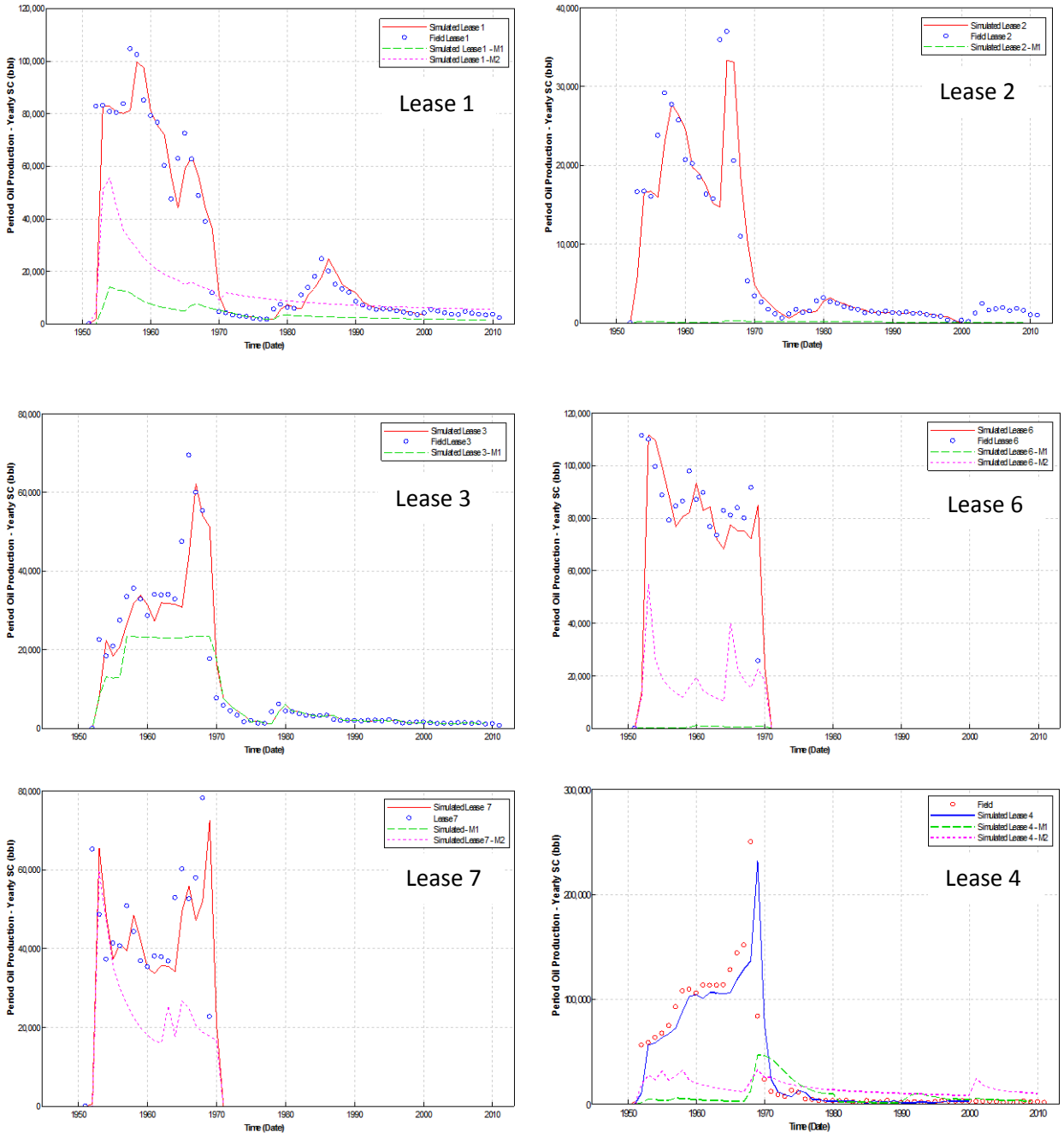

Fig. 4.16 - History match of lease production: simplified model (1 & 2) and integrated model.

4.11 Volumetric Sweep Efficiency.

The Ogallah reservoir was waterflooded since 1952 by an active water drive. At the start of the waterflood, the reservoir pressure was above the bubble point pressure, and there was the volume of gas production was probably enough to run gas engines on the pumping units. We use a technique proposed by Cobb (1997) to compute the volumetric sweep efficiency using oil production. In the waterflood, the volumetric sweep is defined as the fraction of the floodable portion of the reservoir that has been swept by water. The assumption is that all the significant layers, whose permeability and porosity values are greater than the net pay cutoff values, have achieved the fill-up condition. The fill-up condition is determined by the WOR seen in production history undergoing waterflood. All the oil remaining in the reservoir is located in the water swept portion of the reservoir or in the oil bank portion of the reservoir. The volumetric sweep efficiency can be derived based on the above assumptions.

The cumulative waterflood recovery, N_p is the product of original oil-in-place at the start of the waterflood, N, volumetric sweep efficiency, E_{vw}, and displacement sweep efficiency, E_D. E_{vw} is a function of the rock characteristics and E_D is a function of the fluid characteristics. Since the recovery factor (RF) of the waterflood is the ratio N_p to N, the RF is the product of the efficiency, which is a function of the rock properties from different flow units, mobility ratio, pressure distribution and cumulative operations of the wells and the efficiency of the primary depletion.

$$N_p = N \times E_{vw} \times E_D \tag{23}$$

$$\frac{N_p}{N} = RF = E_{vw} \times E_D \tag{24}$$

From the material balance, N_p = (Oil in place at start of waterflooding) – (oil currently in reservoir), so we can show the following.

$$N_p = \frac{V_p S_o}{B_o} - \left[\frac{V_p E_{vw} \left(1.0 - \overline{S_w}\right)}{B_o} + \frac{V_p \left(1.0 - E_{vw}\right)\left(1.0 - S_{wc}\right)}{B_o} \right] \tag{25}$$

Where V_p is the floodable pore volume, B_o is the oil formation volume factor, $\overline{S_w}$ is the average water saturation in the water-swept portion of the pore volume, and S_{wc} is the connate water saturation. Rearranging the eqn. 25 and solving for E_{vw},

$$E_{vw} = \frac{\frac{N_p B_o}{V_p} + (1.0 - S_o - S_{wc})}{\overline{S_w} - S_{wc}} \tag{26}$$

In the oil bank, the S_o is calculated using the formula $S_o = 1.0 - S_{wc}$. For an aquifer with a fairly constant reservoir pressure, the changes in B_o are negligible. For moderate to low mobility ratio waterfloods, $\overline{S_w}$ can be approximated as being a constant as in the case of piston-like displacement. We can approximate the $\overline{S_w}$ by waterflood fractional flow theory as described by Craig (1971,1980) and Willhite (1986). In this case we approximate the $\overline{S_w}$ by $1\text{-}S_{orw}$ where S_{orw} is the waterflood residual oil saturation. Therefore, E_{vw} is defined by a linear relationship with N_p as follows:-

$$E_{vw} = \frac{B_0}{V_p\left(\overline{S_w} - S_{wc}\right)} N_p \tag{27}$$

Table 4.4 provides the reservoir fluid saturations and properties, reservoir pore volume and production of the Ogallah field. At reservoir temperature of 110F, 36 API, R_s of 20 SCF/STB, B_o is about 1.0198 RB/STB with bubble point pressure of 48.26 psi and initial pressure of 1200 psia. Water formation volume factor, Bw for 100,000 ppm salinity is 1.00913 RB/STB. The calculated volumetric sweep efficiency for the Ogallah field is presented in Fig. 4.17.

Table 4.4 – Waterflood data of Ogallah Field		
Description	**Dolomite**	**Sandstone**
Swc	0.369	0.25
Sg	0	0
So	0.631	0.75
Miuo	2	1.5
Sorw	0.25	0.2
Bo , RB/STB	1.0091	1.0091
Vp or pore volume, MB	43286	23497
Cumulative oil production, Np, MSTB	9155.3	2431.8
Current Volumetric Sweep Efficiency. Evw	0.5603	0.1899
Recovery Factor, Rf	0.16	0.16
Displacement Efficiency, Ed	0.2856	0.8426

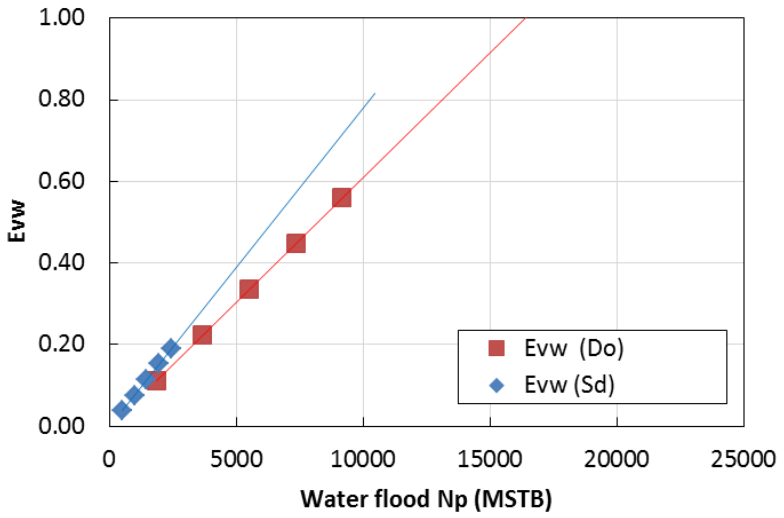

Fig. 4.17 - Volumetric sweep efficiency for Ogallah field.

The main objective of the study was to demonstrate the advantages of conducting an integrated study to describe, model and simulate a reservoir. The PVT properties used to compute the analysis were based on the availability of PVT data provided at the time the study was conducted. The volumetric sweep

efficiency determined from the analysis has shown that the dolomite interval has a better sweep efficiency than sandstone in the Ogallah field. This overall result is believed to be the effect of the operation practice of the reservoir, where the majority of the producing wells were only perforated at the upper zone of about 10 -15 feet , and therefore the contacted volume was mainly from the dolomite intervals.

4.12 Summary

Direct simulation of the integrated model resulted in a good history match without the necessity for optimization methods. In particular, a history match at the field level was achieved simultaneously with the wells. The WOR showed a satisfactory match in all the wells with no adjustment on porosity and permeability, only the relative permeability curves were adjusted. The adjustment in the relative permeability curves was justifiable since the relative permeability curves for each rock type were not available. In this study, application of an integrated approach of reservoir characterization from different sources of data yielded a reservoir description with improvement on the field production data history match with a reasonable primary recovery factor of 16%.

CHAPTER 5

CONCLUSIONS

In this study, we have developed and applied an integrated approach to generate a history matched reservoir model that sufficiently represents reservoir behavior while honoring the geological continuity. We proposed new workflows for characterizing and building the reservoir for a mature field with limited data. Pore structure classification and electrofacies were used together to estimate porosity as well as permeability from well logs while preserving critical heterogeneity in the reservoir rock. In this work, we applied Sequential Gaussian Simulation as a means to populate the reservoir properties and performed history matching using a combination of manual and automatic methods, with minimal alterations to porosity and permeability obtained from reservoir characterization. The history matching was carried out while studying the fluid flow at the field level and at each individual well. The main conclusions can be summarized as follows:

1. Using model-based clustering, the well logs were classified into electrofacies, which were found to correspond closely to lithofacies observed from core descriptions. This enabled us to isolate the heterogeneity arising from different lithofacies.
2. Rock fabric number and Flow zone indicator were identified as suitable petrophysical classifiers to classify the porosity-permeability relationship in sandstone and carbonate respectively.
3. The cementation exponent and petrophysical classifiers were both found to depend on the pore structure of the rock. Classification of pore structure provided the basis to identify porosity-permeability relationships and develop well-core transforms to predict petrophysical properties. This approach was used to generate a porosity-permeability profile and rock types at well locations where core data were not available.
4. Using geostatistics, the estimated information facilitated a fairly accurate reservoir description for reservoir modeling and simulation in a field with limited data. The reservoir model generated captured the characteristics of geological trends and realistic heterogeneities.
5. An integrated reservoir model was developed using the improved reservoir description and compared against simplified models that were built using averaged values of porosity and permeability. History matching results demonstrated that the improved model facilitated a good match for the production data both at field level and individual well level. The simplified models, on the other hand, required porosity and permeability alterations, that violated the geological continuity. The history matching of the Ogallah field using the integrated model yielded a reasonable 15% recovery factor.

REFERENCES

Aanonsen, S. I. 2008. Efficient History Matching Using a Multiscale Technique. *SPE Reservoir Evaluation & Engineering* **11** (1): pp. 154-164. 92758-PA. 10.2118/92758-pa.

Aanonsen, S. I., Nævdal, G., Oliver, D. S., Reynolds, A. C. & Vallès, B. 2009. The Ensemble Kalman Filter in Reservoir Engineering--a Review. *SPE Journal* **14** (3): pp. 393-412. SPE-117274-PA. 10.2118/117274-pa.

Abbaszadeh, M., Fujii, H. & Fujimoto, F. 1996. Permeability Prediction by Hydraulic Flow Units - Theory and Applications. *SPE Formation Evaluation* **11** (4): 263-271. 10.2118/30158-pa.

Al-anazi, A. F. & Gates, I. D. 2010. Support-Vector Regression for Permeability Prediction in a Heterogeneous Reservoir: A Comparative Study. *SPE Reservoir Evaluation & Engineering* (06): 10.2118/126339-pa.

Alpak, F. O. & Kats, F. v. 2009. Stochastic History Matching of a Deepwater Turbidite Reservoir. SPE Reservoir Simulation Symposium. Society of Petroleum Engineers. 01/01/2009. 10.2118/119030-ms.

Amaefule, J. O., Altunbay, M., Tiab, D., Kersey, D. G. & Keelan, D. K. 1993. Enhanced Reservoir Description: Using Core and Log Data to Identify Hydraulic (Flow) Units and Predict Permeability in Uncored Intervals/Wells. SPE Annual Technical Conference and Exhibition. Society of Petroleum Engineers, Inc. 10/03/1993. SPE-26436-MS. 10.2118/26436-MS.

Archie, G. E. 1942. The electrical resistivity log as an aid in determining some reservoir characteristics. *Transactions of the American Institute of Mining and Metallurgical Engineers* **146** 54-61.

Bhattacharya, S., Byrnes, A. P., Watney, W. L. & Doveton, J. H. 2008. Flow unit modeling and fine-scale predicted permeability validation in Atokan sandstones: Norcan East Kansas. *American Association of Petroleum Geologists Bulletin* **92** (Compendex): 709-732.

Breiman, L. & Friedman, J. H. 1985. Estimating Optimal Transformations for Multiple Regression and Correlation. *Journal of the American Statistical Association* **80** (391): 580-598.

Byrnes, A. P., Franseen, E. K. & Steinhauff, D. M. 1999. Integrating plug to well-scale petrophysics with detailed sedimentology to quantify fracture, vug and matrix properties in carbonate reservoirs; an example from the Arbuckle Group, Kansas. University of Kansas, 3.

Caers, J. 2003. History Matching Under Training-Image-Based Geological Model Constraints. *SPE Journal* **8** (3): 218-226. 10.2118/74716-pa.

Caers, J., Hoffman, T., Strebelle, S. & Wen, X. H. 2006. Probabilistic integration of geologic scenarios, seismic, and production data—a West Africa turbidite reservoir case study. *The Leading Edge* **25** (3): 240-244.

Cobb, W. & Marek, F. 1997. Determination of volumetric sweep efficiency in mature waterfloods using production data. Annual Technical Conference and Exhibition. San Antonio, Texas: Society of Petroleum Engineers.

Corbett, P. W. M. & Potter, D. K. 2004. Petrotyping: A basemap and Atlas for Navigating through Permeability and Porosity Data for Reservoir Comparison and Permeability Prediction. *International Symposium of the Society of Core Analysts*

Craig, F. F. 1971,1980. The reservoir engineering aspects of waterflooding. Richardson, TX Society of Petroleum Engineers

Cuddy, S., Allinson, G. & Steele, R. 1993. A Simple, Convincing Model for Calculating Water Saturations in Southern North Sea Gas Fields. SPWLA 34 Annual Logging Symposium. Society of Petrophysicists & Well Log Analysts.

Doll, H., Sauvage, R. & Martin, M. 1952. Application of micrologging to determination of porosity. *Oil and Gas Jour.(September 1)*

Doveton, J. H. 2001. Development of an Archie Equation Model for Log Analysis of Pennsylvanian Oomoldic Zones in Kansas. *KGS Open File Report*. Lawrence.

Emerick, A. A. & Reynolds, A. C. 2011. History Matching a Field Case Using the Ensemble Kalman Filter With Covariance Localization. *SPE Reservoir Evaluation & Engineering* (4): pp. 423-432. 10.2118/141216-pa.

Focke, J. & Munn, D. 1987. Cementation exponents in Middle Eastern carbonate reservoirs. *SPE Formation Evaluation* **2** (2): 155-167.

Frailey, S. M., Damico, J. & Leetaru, H. E. 2011. Reservoir characterization of the Mt. Simon Sandstone, Illinois Basin, USA. *Energy Procedia* **4** 5487-5494. 10.1016/j.egypro.2011.02.534.

Franseen, E. K., A. P. Byrnes, et al. 2004. The Geology of Kansas, Arbuckle Group. Current Research in Earth Sciences. Lawrence, Kansas, University of Kansas. Bulletin 250 - Part 2.

Glover, P. 2009. What is the cementation exponent? A new interpretation. *The Leading Edge* **28** (1): 82-85. 10.1190/1.3064150.

Gomez, C. T., Dvorkin, J. & Vanorio, T. 2010. Laboratory measurements of porosity, permeability, resistivity, and velocity on Fontainebleau sandstones. *Geophysics* **75** (6): E191.

Guerreiro, L., Silva, A. C., Alcobia, V. & Soares, A. 2000. Integrated reservoir characterization of a fractured carbonate reservoir. *paper SPE* **58995**

Guo, G., Diaz, M. A., Paz, F. J., Smalley, J. & Waninger, E. A. 2007. Rock Typing as an Effective Tool for Permeability and Water-Saturation Modeling: A Case Study in a Clastic Reservoir in the Oriente Basin. *SPE Reservoir Evaluation & Engineering* **10** (6): pp. 730-739. 10.2118/97033-pa.

Haro, C. 2010. The Equations Archie Forgot: Anisotropy of the Rocks. *SPE Reservoir Evaluation & Engineering* **13** (5): 823-836.

Hoffman, B. T., Jef, K. C., Xian-Huan, W. & Sebastien, B. S. 2006. A Practical Data Integration Approach to History Matching: Application to a Deepwater Reservoir. *SPE Journal* **11** (4): pp. 464-479. 10.2118/95557-pa.

Hoffman, B. T. & Kovscek, A. R. 2003. Light-Oil Steamdrive in Fractured Low-Permeability Reservoirs. SPE Western Regional/AAPG Pacific Section Joint Meeting. Society of Petroleum Engineers. 01/01/2003. 10.2118/83491-ms.

Huang, N., Aho, G., Baker, B., Matthews, T. & Pottorf, R. 2011. Integrated Reservoir Modeling of a Large Sour-Gas Field With High Concentrations of Inerts. *SPE Reservoir Evaluation & Engineering* **14** (4): 398-412.

Lee, S. H. & Datta-Gupta, A. 1999. Electrofacies characterization and permeability predictions in carbonate reservoirs: Role of multivariate analysis and nonparametric regression. *1999 SPE Annual Technical Conference and Exhibition: 'Formation Evaluation and Reservoir Geology', October 3, 1999 - October 6, 1999*. Houston, TX, USA: Soc Pet Eng (SPE), 409-421.

Lee, S. H., Kharghoria, A. & Datta-Gupta, A. 2002. Electrofacies Characterization and Permeability Predictions in Complex Reservoirs. *SPE Reservoir Evaluation & Engineering* **5** (3): 237-248. 10.2118/78662-pa.

Lucia, F. 1983. Petrophysical parameters estimated from visual descriptions of carbonate rocks: a field classification of carbonate pore space. *Journal of Petroleum Technology* **35** (3): 629-637.

Lucia, F., Kerans, C. & Jennings, J. 2003. Carbonate reservoir characterization. *Journal of Petroleum Technology* **55** (6): 70-72.

Lucia, F. J. 1995. Rock-fabric/petrophysical classification of carbonate pore space for reservoir characterization. *AAPG Bulletin-American Association of Petroleum Geologists* **79** (9): 1275-1300.

Lucia, F. J. 2007. *Carbonate Reservoir Characterization: An Integrated Approach.* Berlin ; New York: Springer.

Mathisen, T., Lee, S. & Datta-Gupta, A. 2003a. Improved Permeability Estimates in Carbonate Reservoirs Using Electrofacies Characterization: A Case Study of the North Robertson Unit, West Texas. *SPE Reservoir Evaluation & Engineering* **6** (3): 176-184.

Mathisen, T., Lee, S. H. & Datta-Gupta, A. 2003b. Improved Permeability Estimates in Carbonate Reservoirs Using Electrofacies Characterization: A Case Study of the North Robertson Unit, West Texas. *SPE Reservoir Evaluation & Engineering* **6** (3): 10.2118/84920-pa.

Mattax, C. & Dalton, R. 1990. Reservoir Simulation (includes associated papers 21606 and 21620). *Journal of Petroleum Technology* **42** (6): 692-695.

Medina, C. R., Rupp, J. A. & Barnes, D. A. 2011. Effects of reduction in porosity and permeability with depth on storage capacity and injectivity in deep saline aquifers: A case study from the Mount Simon Sandstone aquifer. *International Journal of Greenhouse Gas Control* **5** (1): 146-156. 10.1016/j.ijggc.2010.03.001.

Mohaghegh, S., Balan, B. & Ameri, S. 1997. Permeability Determination From Well Log Data. *SPE Formation Evaluation* **12** (3): 10.2118/30978-pa.

Perez, H. H., Datta-Gupta, A. & Mishra, S. 2003. The Role of Electrofacies, Lithofacies, and Hydraulic Flow Units in Permeability Predictions from Well Logs: A Comparative Analysis Using Classification Trees. SPE Annual Technical Conference and Exhibition. 01/01/2003.

Rahmawan, I., Firmanto, T., Priyantoro, J., Kurniawan, A., Rachman, Y. A. & Gomaa, E. 2009. Estimating Permeability in Un-cored Wells Using Modified Flow Zone Index. Asia Pacific Oil and Gas Conference & Exhibition. Society of Petroleum Engineers. 08/04/2009.

Rezaee, M. R., Motiei, H. & Kazemzadeh, E. 2007. A new method to acquire m exponent and tortuosity factor for microscopically heterogeneous carbonates. *Journal of Petroleum Science and Engineering* **56** (4): 241-251. 10.1016/j.petrol.2006.09.004.

Rogers, S. J., Fang, J., Karr, C. & Stanley, D. 1992. Determination of lithology from well logs using a neural network. *AAPG Bulletin (American Association of Petroleum Geologists);(United States)* **76** (5):

Saggaf, M., Nafi Toksoz, M. & Mustafa, H. 2003. Estimation of reservoir properties from seismic data by smooth neural networks. *Geophysics* **68** (6): 1969.

Salem, H. S. & Chilingarian, G. V. 1999. The cementation factor of Archie's equation for shaly sandstone reservoirs. *Journal of Petroleum Science and Engineering* **23** (2): 83-93. 10.1016/s0920-4105(99)00009-1.

Saner, S., Al-Harthi, A. & Htay, M. T. 1996. Use of tortuosity for discriminating electro-facies to interpret the electrical parameters of carbonate reservoir rocks. *Journal of Petroleum Science and Engineering* **16** (4): 237-249. 10.1016/s0920-4105(96)00045-9.

Schiozer, D. J., Netto, S. L. A., Ligero, E. L. & Maschio, C. 2005. Integration of History Matching And Uncertainty Analysis. **44** (7): 10.2118/05-07-02.

Schulze-Riegert, R. W., Krosche, M., Pajonk, O. & Mustafa, H. 2009. Data Assimilation Coupled to Evolutionary Algorithmsâ□”A Case Example in History Matching. SPE/EAGE Reservoir Characterization and Simulation Conference. Society of Petroleum Engineers. 01/01/2009. 10.2118/125512-ms.

Seiler, A., Evensen, G., Skjervheim, J.-A., Hove, J. & Vabø, J. G. 2009. Advanced Reservoir Management Workflow Using an EnKF Based Assisted History Matching Method. SPE Reservoir Simulation Symposium. Society of Petroleum Engineers. 01/01/2009. 10.2118/118906-ms.

Shenawi, S. H., White, J. P., Elrafie, E. A. & El-Kilany, K. A. 2007. Permeability and Water Saturation Distribution by Lithologic Facies and Hydraulic Units: A Reservoir Simulation Case Study. SPE Middle East Oil and Gas Show and Conference. Society of Petroleum Engineers.

Skelt, C. & Harrison, B. 1995. An Integrated Approach To Saturation Height Analysis. *SPWLA 36 Annual Logging Symposium*. Society of Petrophysicists & Well Log Analysts.

Smith, H. D. & Blum, H. A. 1954. Microlaterolog Versus Microlog For Formation Factor Calculations. *Geophysics* **19** (2): 310-320. 10.1190/1.1438001.

Soto, R. B., Garcia, J. C., Torres, F. & Perez, G. S. 2001. Permeability Prediction Using Hydraulic Flow Units and Hybrid Soft Computing Systems. SPE Annual Technical Conference and Exhibition. Copyright 2001, Society of Petroleum Engineers Inc. 09/30/2001.

Subbey, S., Christie, M. & Sambridge, M. 2004. Prediction under uncertainty in reservoir modeling. *Journal of Petroleum Science and Engineering* **44** (1): 143-153.

Taware, S. V., Taware, A. G., Sinha, A. K., Jamkhindikar, A., Talukdar, R. & Datta-Gupta, A. 2008. Integrated Permeability Modeling Using Wireline Logs, Core and DST Data in a Deepwater Reservoir. SPE Indian Oil and Gas Technical Conference and Exhibition. 01/01/2008.

Teh, W., Willhite, G. P. & Doveton, J. H. 2012. Improved Reservoir Characterization in the Ogallah Field using Petrophysical Classifiers within Electrofacies. SPE Improved Oil Recovery Symposium. Society of Petroleum Engineers. 14-18 April 2012. 10.2118/154341-ms.

Teh, W. J., Willhite, G. P., Doveton, J. H. & Tsau, J.-S. 2011. Improved Predictions of Porosity from Microresistivity Logs in a Mature Field through Incorporation of Pore Typing. SPE Eastern Regional Meeting. Society of Petroleum Engineers. 01/01/2011. 10.2118/149506-ms.

Thiele, M. R., Batycky, R. P. & Fenwick, D. H. 2010. Streamline Simulation for Modern Reservoir-Engineering Workflows. *SPE Journal of Petroleum Technology* (1): 64-70. 10.2118/118608-ms.

Todd Hoffman, B. & Caers, J. 2005. Regional probability perturbations for history matching. *Journal of Petroleum Science and Engineering* **46** (1-2): 53-71. DOI: 10.1016/j.petrol.2004.11.001.

Vasco, D., Seongsik, Y. & Akhil, D. G. 1999. Integrating dynamic data into high-resolution reservoir models using streamline-based analytic sensitivity coefficients. *SPE Journal* **4** (4): 389-399.

Verwer, K., Eberli, G. P. & Weger, R. J. 2011. Effect of pore structure on electrical resistivity in carbonates. *AAPG BULLETIN* **95** (2): 175.

Winsauer, W. O., Shearin, H., Masson, P. & Williams, M. 1952. Resistivity of brine-saturated sands in relation to pore geometry. *Bulletin of the American Association of Petroleum Geologists* **36** (2): 253-277.

Willhite, G. P. 1986. *Waterflooding*. Richardson TX: Society of Petroleum Engineers.

Yang, A. P. 1997. Integrated reservoir description from seismic, well log, to production data.

Yang, C., Nghiem, L. X., Card, C. & Bremeier, M. 2007. Reservoir Model Uncertainty Quantification Through Computer-Assisted History Matching. SPE Annual Technical Conference and Exhibition. Society of Petroleum Engineers. 11/11/2007.